

**AXIAL AND REFLECTION ASYMMETRY  
OF  
THE NUCLEAR GROUND STATE\***

P. MÖLLER

Theoretical Division, Los Alamos National Laboratory  
Los Alamos, NM 87545

R. BENGTSSON, B. G. CARLSSON, and P. OLIVIUS

Department of Mathematical Physics, Lund Institute of Technology,  
P. O. Box 118, SE-22100 Lund, Sweden

T. ICHIKAWA

RIKEN Nishina Center, RIKEN, Wako, Saitama, 351-0198, Japan

H. SAGAWA

Center for Mathematical Sciences, University of Aizu  
Aizu-Wakamatsu, Fukushima 965-80, Japan

and

A. IWAMOTO

Japan Atomic Energy Agency (JAEA), Tokai-mura, Naka-gun, Ibaraki, 319-1195, Japan

ATOMIC DATA AND NUCLEAR DATA TABLES, **94** (2008) 758–780

September 14, 2007

Revised November 7, 2007 and June 23, 2008

More than a decade ago we published a calculation of nuclear ground-state masses and deformations in ATOMIC DATA AND NUCLEAR DATA TABLES [**59**,185 (1995)]. In that study, triaxial nuclear shapes were not considered. We have now enhanced our model and studied the influence of triaxial shape degrees of freedom on the nuclear ground-state potential energy (mass) and ground-state shape. It turns out that a few hundred nuclei are affected to a varying degree with the largest effect, about 0.7 MeV, occurring near  $^{108}\text{Ru}$ . We here provide a table of the calculated effects of triaxial shape degrees of freedom. Although axial-asymmetry effects were not considered in the 1995 mass calculation, it did study the effects of reflection-asymmetric shape degrees of freedom ( $\epsilon_3$ ) on nuclear masses. However, the magnitude of the effect was not tabulated. Here we provide such a table. In addition we calculate the effect in a much improved fashion: we search a 4-dimensional deformation space ( $\epsilon_2$ ,  $\epsilon_3$ ,  $\epsilon_4$ , and  $\epsilon_6$ ). This is now possible because the computational resources available to us today are more than 100 000 times better than at the time we calculated the mass table published in 1995.

\*This paper is dedicated to the memory of our friend, colleague, and collaborator George A. Leander who in the 1980's made so many important contributions to the studies of axial and reflection asymmetry in the nuclear ground state.

## Contents

<b>1 INTRODUCTION</b>	<b>2</b>
1.1 Which Minimum is the Ground State? . . . . .	3
<b>2 AXIAL ASYMMETRY IN THE NUCLEAR GROUND STATE</b>	<b>4</b>
<b>3 REFLECTION ASYMMETRY IN THE NUCLEAR GROUND STATE</b>	<b>5</b>
<b>4 DISCUSSION</b>	<b>6</b>
4.1 Triaxiality in the Nuclear Ground State . . . . .	6
4.2 Reflection Asymmetry in the Nuclear Ground State . . . . .	9
<b>5 APPENDIX</b>	<b>10</b>
<b>EXPLANATION OF TABLE 1</b>	<b>13</b>
<b>TABLE 1.</b> Calculated Ground-State Axial-Asymmetry Properties	<b>14</b>
<b>EXPLANATION OF TABLE 2</b>	<b>20</b>
<b>TABLE 2.</b> Calculated Ground-State Reflection-Asymmetry Properties	<b>21</b>
<b>EXPLANATION OF GRAPHS</b>	<b>24</b>
<b>GRAPH 1</b> Four Calculated Potential-Energy Surfaces	<b>25</b>
<b>GRAPH 2</b> Nuclear Chart with Ground-State Triaxiality Corrections	<b>26</b>
<b>GRAPH 3</b> Nuclear Chart with Ground-State Reflection-Asymmetry Corrections	<b>27</b>
<b>GRAPH 4</b> Twelve Calculated Potential-Energy Surfaces from $^{98}\text{Ru}$ to $^{120}\text{Ru}$	<b>28</b>

## 1 INTRODUCTION

In a previous issue of ATOMIC DATA AND NUCLEAR DATA TABLES we presented a calculation of nuclear ground-state masses and deformations for 8979 nuclei ranging from  $^{16}\text{O}$  to  $^{339}136$  and extending from the proton drip line to the neutron drip line [1]. The calculation was based on the macroscopic-microscopic approach. The microscopic corrections were obtained from levels calculated in a folded-Yukawa single-particle potential [2] by use of the Strutinsky method [3, 4]. Residual pairing corrections were calculated in the Lipkin-Nogami approximation [5, 6, 7, 8]. Two 1992 mass tables were provided, both with this microscopic correction, but with the macroscopic contribution to the total potential energy obtained in two different liquid-drop-type models, namely the finite-range droplet model, and the finite-range liquid-drop model. We refer to the macroscopic-microscopic model in which the total potential energy is calculated as a sum of microscopic corrections from folded-Yukawa single-particle levels and a macroscopic energy term from the finite-range droplet model as the FRDM. The potential-energy model in which the macroscopic term is given by the finite-range liquid-drop model are referred to as the FRLDM. If present, a year in brackets refers to the year the constants and other features of a particular “edition” of the model were determined and frozen. Publication of an edition may not take place until several years later due to the lengthy publication process. For example, the FRDM(1992) appeared in print in 1995 [1].

For historical reasons and for compatibility with previous calculations we use the Nilsson perturbed-spheroid  $\epsilon$  shape parameterization. Its complete specification, including axial asymmetry is quite lengthy and is given in our mass paper [1]. We use the FRLDM model in our calculations here. Because the calculation of fission barriers was much improved relative to the calculations used when the FRLDM(1992) parameter set was determined, we recently redetermined the FRLDM parameters [9]. This most recent model/parameter set we refer to as FRLDM(2002). It is this version that we use here. However, for the results given here the slight difference in model

parameters between the FRLDM(1992) and FRLDM(2002) are unimportant for  $\Delta E_\gamma$  and  $\Delta E_{\epsilon_3}$ ; the two parameter choices give results that are very similar. The parameter differences are mainly important for fission-barrier heights.

Axial asymmetry was not implemented in the computer codes at the time of our mass paper, but this has now been accomplished. A couple of misprints relating to axial asymmetry that occur in some of the equations in Ref. [1] (but which have not migrated to any calculations) are enumerated and corrected in the Appendix. We present here in Table I the detailed results of the first global calculation of the effect of triaxiality on the nuclear ground-state shape and mass. When the calculated binding energy is affected by more than 10 keV by triaxiality we tabulate in Table I the magnitude of the effect and the values of the deformation parameters  $\epsilon_2$ ,  $\epsilon_4$ , and  $\gamma$ . An overview of these results has recently been presented in Ref. [10].

The effect of reflection-asymmetric shape degrees of freedom on nuclear masses was taken into account in the mass calculation presented in Ref. [1] but how much the ground-state energy was lowered by reflection-asymmetric shape degrees of freedom relative to calculations restricted to reflection-symmetric shapes was not presented in tabular form. We now present in Table II the magnitude of the effect, determined in an improved way, from minimization of the potential energy in a full 4-dimensional deformation space in the coordinates  $\epsilon_2$ ,  $\epsilon_3$ ,  $\epsilon_4$ , and  $\epsilon_6$  and the calculated values of those coordinates.

The effect  $\Delta E_\gamma$  on the ground-state potential-energy surface due to axial asymmetry is defined as the difference

$$\Delta E_\gamma = \min_{\epsilon_2, \epsilon_4} E(\epsilon_2, \epsilon_4, \gamma = 0) - \min_{\epsilon_2, \epsilon_4, \gamma} E(\epsilon_2, \epsilon_4, \gamma) \quad (1)$$

Similar definitions and considerations hold for  $\Delta E_{\epsilon_3}$ .

## 1.1 Which Minimum is the Ground State?

Surprisingly it is for heavy nuclei non-trivial to determine which of the many minima in the calculated multi-dimensional potential-energy surface should represent the nuclear “ground state.” To illustrate this, let us consider a double-peaked heavy-element fission barrier. In a calculation we obtain with increasing elongation of the nuclear shape: a ground-state minimum, a first barrier peak, a fission-isomeric minimum, and an outer barrier peak. For a nucleus such as  $^{238}\text{U}$ , for example, the calculated fission-isomeric minimum is 2 to 3 MeV higher than the ground-state minimum. However, for some heavy nuclei we may obtain a first barrier peak 6 MeV above the first minimum, a fission isomeric minimum with an energy 1 MeV *below* the first minimum and an outer barrier peak 2 MeV higher than the fission isomeric minimum. To choose the ground state as  $\min_{\epsilon_2, \epsilon_4, \gamma} E(\epsilon_2, \epsilon_4, \gamma)$  would mean that the fission isomer would be considered the ground state and that its mass would be entered into the mass table. However, because of the low barrier this configuration would have such a short fission half-life that it would be difficult to observe. In contrast, this nucleus would have a long fission-decay half-life in the first, slightly higher minimum. It is therefore more natural to consider the first minimum as the “ground state” of this nucleus.

No ambiguity in identifying the ground-state minimum in calculated potential-energy surfaces will arise if we define the nuclear ground state as the minimum with the highest barrier with respect to fission. We are able to identify this minimum by use of immersion techniques in our calculated multi-dimensional potential-energy landscapes [11]. It is this minimum we tabulate in a mass table and use as the ground state. However, it is not possible to define  $\Delta E_\gamma$  for some nuclei with  $N \geq 160$  because it is not clear it should be defined with respect to  $\min_{\epsilon_2, \epsilon_4} E(\epsilon_2, \epsilon_4, \gamma = 0)$  for nuclei with complex potential-energy surfaces. We have checked that for nuclei with  $N < 160$  the two methods for selecting which of several minima is the ground state yield identical results, except for  $^{232}\text{No}$ . However, for this nucleus the ground-state mass is not decreased by triaxiality. Therefore we can unambiguously define  $\Delta E_\gamma$  for the region of the nuclear chart tabulated in Table I. For  $N \geq 160$  it is still straightforward to determine which minimum is the ground state and the corresponding

nuclear ground-state mass, although it is more difficult, and in some cases impossible, to find a natural definition of  $\Delta E_\gamma$ . Therefore we must limit the tabulation in Table I to nuclei with  $N < 160$ .

## 2 AXIAL ASYMMETRY IN THE NUCLEAR GROUND STATE

In our computer model most of the time is used to calculate the single-particle levels. Once the levels are determined the time to calculate the shell corrections and macroscopic contributions to the potential energy is almost negligible. The same set of levels can be used to calculate the shell correction for several neighboring nuclei to satisfactory accuracy. However, excursions too far away would lead to inaccuracies because the single-particle well radius changes with the size of the system and other parameters such as the spin-orbit strength also vary slowly with nuclear size. We consider nuclei between the neutron and proton drip lines from  $A = 31$  to  $A = 330$ . We divide this region into 45 different subregions, each of which is sufficiently limited so that within each subregion the shell corrections can be calculated from the same set of single-particle levels. These subregions are defined by first selecting larger regions of the nuclear chart, namely from  $A = 31$  to  $A = 50$ ,  $A = 51$  to  $A = 70$  and so on, with each section 20 nucleons wide. We then subdivide each of these regions into 3 parts: a region on the proton-rich side of  $\beta$  stability, a region corresponding to  $\beta$ -stable and near- $\beta$ -stable nuclei, and a third region consisting of neutron-rich nuclei. For each of these 45 subregions we calculate the energy for each nucleus for the deformation grid  $\varepsilon_2 = (0.0, 0.025, \dots, 0.45)$ ,  $\gamma = (0.0, 2.5, \dots, 60.0)$ , and  $\varepsilon_4 = (-0.12, -0.10, \dots, 0.12)$ , altogether 6175 grid points. So that we can determine, when multiple minima are present in the calculated potential-energy surfaces, which of these minima has the highest barrier with respect to fission, we extend the calculations to  $\varepsilon_2 = 0.75$  for  $A > 170$ . For lighter nuclei the correct ground state is always obtained by using the simpler criterion that the lowest minimum should be designated as the ground state. In practice we calculate each subregion on a separate CPU in our computer cluster. The three-dimensional potential-energy space of each nucleus is then analyzed by immersion techniques and all minima and all saddle points are identified.

As a final step we generate potential-energy contour plots of all systems. The contour maps have been constructed in the following way. In each point  $\varepsilon_2$  and  $\gamma$  we display the lowest energy obtained for the 13  $\varepsilon_4$  grid points calculated. We have previously strongly emphasized that such a procedure in general does not give reasonable results in, for example, situations where the surface contains multiple local minima versus  $\varepsilon_4$  and in some other situations [11, 9]. However, we use the method for the purpose of overview illustration only. All our specific results on minima and separating saddle points are obtained from a complete and appropriate immersion analysis of the full 3D space. These data are written onto a file, which is then read by the plotting program which inserts the location of the minima and saddle points in the contour plots. The minima in the plots are shown as dots and the saddle points as X symbols. We show four representative contour plots in Graph 1. Here we are only interested in the axially asymmetric minima. However, other interesting situations occur. For example, oblate-prolate shape isomers and other types of shape isomers. They will be the subject of another paper.

In our calculations we use the same set of single-particle levels to calculate the shell-plus-pairing corrections for several nearby nuclei. We take one additional step to enhance accuracy after the minima and separating saddle points have been determined. The deformations and energies of all these stationary points were written by the immersion analysis program onto a file. The energies at these deformations are then recalculated with the precise model parameters for the nucleus under consideration. Some quantities that depend on  $Z$  and  $N$  are the single-particle potential radii and depths, the strength of the spin-orbit force and the pairing strength which are all smoothly and slowly varying functions of  $Z$  and  $N$ . Thus, in the recalculation these quantities assume exactly their proper values for this nucleus and the shell-plus-pairing corrections are calculated from the precise levels obtained. This strategy is based on the assumption that the locations of minima or saddles are less sensitive to parameter variations than the energy itself. We have performed

numerous checks of this assumption and it is fulfilled to a very high degree. We used the same procedure to calculate the FRDM(1992) and FRLDM(1992) mass tables [1].

For nuclei whose ground states are affected by axial asymmetry we determine how much the axial-asymmetry shape degree of freedom lowers the ground-state energy relative to the minimum energy that is obtained in calculations restricted to axial symmetry. These results are given in Table I and Graph. 2. When reviewing the results on axial asymmetry we observe that near  $Z = 44$  the effect of axial asymmetry changes very suddenly near  $Z + N = A = 110$ . This is exactly where we change parameters from a strip  $A = 91 \rightarrow 110$  to  $A = 111 \rightarrow 130$  and the rapid drop-off could be due to a change of parameters. Therefore we have recalculated nuclei in this region for parameters appropriate for a strip  $A = 106 \rightarrow 115$  (so there is no discontinuity in model parameters across the  $A = 110$  line) and use that calculation in this specific region. But no significant effect on the results was observed. We still obtain an abrupt disappearance of axial asymmetry near  $A = 110$  and a reemergence near  $A = 120$ . A suite of computer programs and scripts has been developed to perform the immersion analysis, plot the potential-energy graphs, generate the tables, and other related steps in this procedure in a highly automated fashion.

For a discussion on how our results on axial asymmetry compare to experimental data we refer to the recent paper [10].

### 3 REFLECTION ASYMMETRY IN THE NUCLEAR GROUND STATE

In our mass calculation [1] the determination of the ground-state mass proceeded in the following way. In the initial step the potential energy was calculated as a function of  $\epsilon_2$  and  $\epsilon_4$ . The ground-state minimum was identified in this space and the values of the shape coordinates  $\epsilon_2$  and  $\epsilon_4$  were tabulated. Then, for each nucleus, two further minimizations were carried out, both with  $\epsilon_2$  and  $\epsilon_4$  held fixed at their previously determined values. In one of the minimizations the energy was minimized with respect to  $\epsilon_3$ , in the other  $\epsilon_6$  was varied (with  $\epsilon_3 = 0$ ). The lowest of the two minima obtained was tabulated as the ground state.

Here we considerably refine this calculation. In 1987, when we performed the first step in our mass calculation, namely the calculation of the potential-energy surfaces versus  $\epsilon_2$  and  $\epsilon_4$  we saved (and have retained ever since) these simple potential-energy surfaces and a table of *all* minima found in these surfaces. Here we study the stability of all these minima in a full 4D deformation space in the coordinates  $\epsilon_2$ ,  $\epsilon_3$ ,  $\epsilon_4$  and  $\epsilon_6$ . We use a grid with a grid-point distance of 0.01 in all 4 deformation parameters. We start by calculating a 4D “hyper-cube” around the minimum found in the 2D  $\epsilon_2$ - $\epsilon_4$  space. Such a hyper-cube consists of 81 grid points, 80 of them on the surface of the hyper-cube. The lowest energy will be a grid point on the surface of this hyper-cube, unless the initial point determined from the limited 2D calculation accidentally turns out to be the location of the local minimum. If not, we construct a new 4D hyper-cube around the grid point corresponding to the lowest energy on the surface of the initial hyper-cube, taking care not to recalculate energies that are already calculated. We continue in this fashion until the lowest-energy point is *not* on the surface of the last hyper-cube investigated. It is then the interior point in this last hyper-cube that is the minimum in the full 4D space. We investigate all the minima found in the 2D space in this fashion. However, we find that sometimes there exists one minimum for  $\epsilon_3 = 0$  and another at  $\epsilon_3 \approx 0.1$ , separated by a low ridge. We therefore repeat the search for minima with the above starting points, except  $\epsilon_3 = 0.1$  in all the starting points. The lowest of the 4D minima is the optimum choice for the ground state.

We now do a completely analogous calculation but in a 3D space, with  $\epsilon_3$  set to zero. We identify the lowest minimum in this space. The difference between the minimum energies in the 3D and 4D spaces we tabulate as  $\Delta E_{\epsilon_3}$  in Table II and Graph 3.

This approach improves the accuracy of our original study for two reasons. First, in the original study we only investigated one minimum with respect to higher multipole deformations, namely

the lowest minimum found in the 2D  $\epsilon_2$ - $\epsilon_4$  space. However, if another minimum, a shape isomer, exists in the 2D  $\epsilon_2$ - $\epsilon_4$  space then, if the effect of varying  $\epsilon_3$  and  $\epsilon_6$  is investigated for both these minima, it may turn out that the higher of the original minima becomes the lower minimum after the full variation of the four deformation parameters. Second, we perform a completely independent variation of the four deformation parameters in a full 4D deformation space, rather than the very restricted variation that was the only tractable computation possible more than a decade ago.

For a discussion on how our results on reflection asymmetry compare to experimental data we refer to Refs. [12, 13, 14].

## 4 DISCUSSION

Determining the ground-state shapes of nuclei has been a very active research field for more than 50 years, ever since it became clear in the 1950's that nuclei are not always spherical in their ground states but may be oblate or prolate in shape. Later, interest expanded to other types of symmetry-breaking shapes, in particular reflection-asymmetric and triaxial ground-state shapes of nuclei. Apart from our studies there are no global studies covering the whole nuclear chart within a consistent model framework of such effects. However, many studies of these effects in limited regions of nuclei have been performed previously in a variety of models. No consistent picture emerges from those studies, but in some of the studies there are similarities with our current results. Triaxiality in nuclei has mostly been studied in rotating nuclei. A recent review of symmetry breaking in rotating nuclei is in Ref. [15]. An extensive review of reflection asymmetry in the nuclear ground state is Ref. [16]; more limited discussions of triaxiality and reflection asymmetry in the nuclear ground state are given in Refs. [14, 17, 18]. Because of the availability of extensive reviews we here restrict ourselves to a discussion of how a few representative earlier calculations in limited regions of the nuclear chart compare to our current global investigation.

### 4.1 Triaxiality in the Nuclear Ground State

Perhaps the first comprehensive study of axial asymmetry in the nuclear ground state over a larger region of nuclei is the 1969 study of the “neutron-deficient rare-earth region”, that is  $50 < Z, N < 82$  by Arseniev, Sobczewski, and Soloviev [19]. They state in their conclusions: *Thus, the equilibrium shapes are axially symmetric*. However, this is contrary to our current results where we find strong effects of axial asymmetry at  $N = 76$ , in agreement with experimental results and some more recent theoretical studies, see discussion in [10]. In addition they find  $^{126}\text{Ba}$  to be oblate in the ground state, whereas we find that the conditional oblate minimum is 1.5 MeV higher than the prolate ground state. These differences are probably due to unsuitable Nilsson single-particle parameters ( $\kappa$  and  $\mu$ ), the calculation of the potential energy by summing the oscillator single-particle levels, a method we now know is deficient [3, 4, 20, 21], rather than by the Strutinsky shell correction method [3, 4], and to a lesser degree, the non-consideration of hexadecapole shape degrees of freedom in [19]. A subsequent paper by the same authors [22] looks at axial asymmetry in the  $A \approx 100$  region, again with a negative result. But this paper suffers from the same deficiencies as the rare-earth-region study.

Somewhat later Götz and collaborators considered triaxial shape degrees of freedom in the nuclear ground state [23, 24, 25]. In the study [24] of nuclei just “southwest” of  $^{208}\text{Pb}$ , that is nuclei with  $Z < 82, N < 126$ , no triaxial minima are found. For W and Os this is in agreement with our findings. For  $^{194}\text{Pt}$  for which they show a contour diagram, and for which they obtain a weakly oblate ground state we obtain a triaxial ground state, as we also do for many other Pt and Au nuclei. In their later more ambitious paper [25] there is only weak evidence for triaxiality for  $^{130}\text{Cs}$ ,  $^{132}\text{Cs}$ ,  $^{128}\text{Ba}$ , and  $^{130}\text{Ba}$ . This is somewhat in contrast to our results where we find the largest effect for  $N = 76$ , not for  $N = 72$ , as is apparently obtained in [24]. For the heavier rare-earth elements the calculation does not extend sufficiently far towards the proton-rich side to

include  $N = 76$ . A problem with these calculations, much discussed at the time, is the much too bound doubly-magic  $^{208}\text{Pb}$ . This “problem” has never existed in global mass calculations based on the folded-Yukawa single-particle potential [26, 27, 28, 29].

In a study by Larsson *et al.* [30] the onset of triaxiality of the nuclear ground state along a sequence of Pt isotopes, at  $^{190}\text{Pt}$  agrees with our results in Table 1, but triaxiality disappears slightly sooner, already at  $^{194}\text{Pt}$  in [30] whereas we find some effect remains until  $^{195}\text{Pt}$ .

We find in our calculations across the nuclear chart the largest effect of triaxial deformations on the energy of the nuclear ground state for  $^{108}\text{Ru}$  and nearby nuclei, that is for some nuclei in the  $A \approx 100$  region. Faessler *et al.* [31] considered triaxial effects on nuclei in this region. This calculation shows very interesting agreement with our results, to the extent we can compare the calculations. The calculation of Faessler *et al.* does not provide the magnitude of the effect of triaxiality on the nuclear ground-state energy, nor does it include sufficiently many nuclei that we can establish how high in neutron number they find triaxial ground states for the very interesting isotope chains Mo and Ru. But when we compare our Table 1 here and their Table 2a in [31] we find substantial similarities between our results. In terms of  $Z$  significant effects start to occur at  $Z = 42$  and above. For Mo and Ru axial asymmetry starts to become important at  $A = 98\text{--}100$  in both calculations. In our calculation there is no effect beyond  $A = 109$  for Mo and  $A = 111$  for Ru. There is again an effect of triaxiality setting in at about  $A = 116$  in our calculation. The Faessler calculation does not include these neutron-rich nuclei. For Pd we see an effect of triaxiality in the range  $107 \leq A \leq 111$ , Faessler (only even nuclei are considered) for  $A = 106, 108$ , and 110.

A later study by Skalski and collaborators [18] also looks at triaxiality in the  $A \approx 100$  region near  $^{108}\text{Ru}$ . Potential-energy surfaces are calculated by use of two different pairing models, namely a PNP (particle-number-projection) pairing model and a BCS pairing model. The results obtained in the PNP approach appear very similar to our results. For example, for  $^{108}\text{Ru}$  the decrease in potential energy due to triaxiality is about 0.7 MeV and  $\gamma = 19.9$ , in close agreement with 0.63 MeV and  $\gamma = 25.0$  in Table 1. In contrast, their results with the BCS pairing model are quite different, with little effect from triaxiality on the ground-state energy, about 0.2 MeV.

Skalski’s results seem to indicate that the choice of pairing model is crucial. We have therefore calculated the decrease in ground-state mass due to triaxiality for  $^{108}\text{Ru}$  when we use our implementation of the BCS pairing model, as defined in Ref. [8] and with the constants specified there. We find a decrease due to triaxiality of 0.46 MeV, 73% of the effect found in the Lipkin-Nogami pairing model and significantly larger than found by Skalski [18]. Therefore, how crucial is the choice of pairing model?

Olofsson<sup>1</sup> and collaborators [32] have shown that the fluctuating part of the pairing energy (i.e. the pairing-correction energy) is for all practical purposes the same in the BCS and PNP models, provided that the same pairing strength is used and the pairing-correction energies for odd systems are calculated as described by Olofsson [32]. Thus, if the smooth part of the pairing energy is subtracted out and compensated for by a pairing-related term in the macroscopic energy, the choice of pairing model makes little difference for the total energy, implying that we get the same energy surfaces, masses and odd-even mass differences. This applies also to the Lipkin-Nogami pairing model. However, the self-consistent pairing gap, calculated with the same pairing strength, depends on the pairing model, being larger in the PNP model than in the BCS model.

The often-made claim that the BCS and PNP pairing models give different results is based on a misconception, namely that the self-consistent pairing gap should be identified with the experimental odd-even mass difference and that the pairing strength should be adjusted so that the self-consistent pairing gap reproduces the experimental odd-even mass difference. Done this way a larger pairing strength is required in the BCS pairing model than in the PNP pairing model. As a result, the pairing shell energy is different in the two models, leading to differences in energy surfaces, masses and odd-even mass differences as exemplified by Skalski’s calculations.

A large number of experiments have over the years looked at the level structure of nuclei in

---

<sup>1</sup>Olofsson is known as Uhrenholt after September 2, 2007

the  $A \approx 100$  region, for example Refs. [33, 34, 35, 36, 37]. In particular the later studies have very complete data for very neutron-rich Ru isotopes, up to  $^{112}\text{Ru}$ . Low-lying  $\gamma$  bands are seen in the data also in the most neutron-rich isotopes, although we obtain axially symmetric ground states for  $^{112}\text{Ru}$  (oblate shape) as is obtained in the HFB potential-energy surface shown in Fig. 8 in the study by Äystö *et al.* [35], where the ground state is prolate. In both calculations the potential is much softer in the  $\gamma$  direction for  $^{112}\text{Ru}$  than for  $^{108}\text{Ru}$ . In our calculation the triaxial ground state of  $^{108}\text{Ru}$  is much more strongly established than in the calculation of Äystö *et al.* [35]. We show in Graph 4 how the properties of the potential-energy surface evolve for a sequence of twelve even Ru isotopes from  $^{98}\text{Ru}$  to  $^{120}\text{Ru}$ .

Additional calculations on triaxiality of the nuclear ground state have appeared over the years but no very consistent picture emerges from these calculations which employ a variety of macroscopic-microscopic potentials or self-consistent HFB models with Skyrme forces. The lack of a consistent picture can be expected, since none of these calculations (with one exception, see below) has been benchmarked in a global calculation of nuclear masses and deformations, in contrast to the model presented here, which has been applied to global calculations in successively enhanced versions for more than 25 years [27, 28, 1]. However, there is one area of substantial consensus: most calculations find that triaxial shapes are important in the neutron-deficient rare-earth region with a maximum effect at  $N = 76$ , as we do here. In their early work, based on a Nilsson modified oscillator single-particle potential, Ragnarsson and collaborators [38] find an effect at  $N = 76$  with a maximum at  $Z = 62\text{--}64$ , in agreement with our results. However, hexadecapole deformations are not included in the  $\gamma$  plane in Ragnarsson's calculations. Girod and Grammaticos [39] studied six nuclei with respect to axial asymmetry in an HFB model. There is an almost complete non-overlap with their results and our results here; we only agree that  $^{134}\text{Ce}$  has a static triaxial ground-state shape. A later more extensive study was published in 1983 [40]. In their study of some proton-rich rare-earth nuclei Redon *et al.* [41] find triaxial ground states in the vicinity of  $N = 76$  for Sm, but none for Cd, in qualitative agreement with our results. In a more comprehensive study Kern *et al.* [42] study the behavior of light rare-earth level spectra and how they evolve in the range  $132 \leq A \leq 140$ . They find that the level spectra for some of these nuclei are best understood in terms of potential-energy surfaces with well-established triaxial minima. For these nuclei they also find that static potential-energy surfaces obtained in calculations based on their macroscopic-microscopic model with a Woods-Saxon single-particle potential exhibit such well-established triaxial ground states.

In 2000 Dutta, Pearson, and Tondeur calculated ground-state shapes in the ETFSI method in an implementation that allowed triaxial nuclear shapes [43]. Earlier, this ETFSI model, restricted to axially symmetric shapes, had been used in global calculations of nuclear ground-state masses by Aboussir *et al.* [44]. Since this is the only study of triaxial nuclear ground-state shapes in a microscopic model that has been benchmarked in a global nuclear mass calculation, it is of considerable interest to compare with our results. However, one should note that the study of triaxial nuclear ground-state shapes by Dutta *et al.* is not global, it is limited to 36 relatively randomly selected nuclei; in contrast we study almost 9000 nuclei. The authors find that out of the 36 nuclei they study 32 are triaxial in their ground states. This preponderance of triaxial ground-state shapes is unanticipated and seems to be contradicted by experimental level-structure data [10]. The authors conjecture that they obtain triaxial shapes in so many cases just as a compensation for a too limited axially-symmetric deformation space, namely only two deformation parameters ( $c, h$ ). To test this conjecture they study what happens in their model if they release the constraint of reflection asymmetry, but retain axial symmetry. They find that in most cases the nuclei remained right-left symmetric. They summarize with the comment: “*We are thus inclined to accept the widespread occurrence of triaxiality that we find as being an essential feature of ETFSI calculations, if not of the real world.*” In contrast, in our work about an equal number of nuclei are affected by axial and reflection asymmetry, which seems to be more consistent with real-world observations [10]. One point of similarity between our results is that in the calculations by Dutta *et al.* [43] axial asymmetry lowers the nuclear ground state by a maximum of 0.7 MeV with respect to

minima found in calculations restricted to axial symmetry, in agreement with the maximum effect we find.

## 4.2 Reflection Asymmetry in the Nuclear Ground State

Because of the long-known low-lying negative-parity states in nuclei near  $^{222}\text{Ra}$  many limited theoretical studies on octupole effects have been presented previously. Early attempts to find non-zero equilibrium octupole deformations in this region of the nuclear chart were negative. Vogel calculated potential-energy surfaces by summing Nilsson modified-oscillator single-particle levels but found no instability with respect to octupole deformations [45]. In a similar study based on the same Nilsson potential, but with the potential-energy surfaces calculated by use of the just developed macroscopic-microscopic method [3, 4, 20] only a few nuclei were subject to a weak octupole instability for oblate shapes [46]. Later Neergård and Vogel developed a model in which they described the low-lying negative parity states in terms of octupole vibrations [47, 48].

A turning-point in the studies of octupole effects in the nuclear ground state were the results obtained in the FRLDM (1981) study of nuclear masses by Möller and Nix [12]. In this study ground-state shapes and masses were determined by minimizing the nuclear potential energy with respect to  $\epsilon_2$  and  $\epsilon_4$  shape degrees of freedom. Additional shape degrees of freedom were not taken into account due to the computational limitations at that time. It was observed that some of the largest differences between calculated and experimental nuclear ground-state masses in the nuclear chart were centered at  $^{222}\text{Ra}$  and that this correlated well with the experimental observations that the negative-parity states observed in experiments had their lowest energies near  $^{222}\text{Ra}$ . A calculation of octupole deformations on the nuclear ground state was performed for five sample nuclei, namely  $^{91}\text{Kr}$ ,  $^{184}\text{Hf}$ ,  $^{218}\text{Ra}$ ,  $^{222}\text{Ra}$ , and  $^{224}\text{Ra}$ . An effect was found only for  $^{222}\text{Ra}$  and  $^{224}\text{Ra}$  for which the consideration of octupole deformations decreased the discrepancy between calculated and experimental masses from 1.81 MeV to 0.11 MeV and 1.43 MeV to 0.41 MeV, respectively.

These results gave the impetus to a large number of new theoretical and experimental studies, for example [13, 49] and the very comprehensive work by Leander and Chen [14], which also contains large number of references to experimental and theoretical work. In [14] Leander and Chen modeled the low-energy spectroscopy of odd- $A$  nuclei in the mass region  $A \approx 219\text{--}229$  by coupling states of a deformed shell model, including octupole deformation, to a reflection-asymmetric rotor core. In their conclusions they summarize: *The description of experimental data was optimized for each nucleus with respect to  $\beta_3$ . The fact that this optimization invariably favored or allowed a nonzero  $\beta_3$  leaves little doubt about the role of some sort of surface octupole mode in the  $A \approx 219\text{--}229$  region.* Furthermore, in the abstract they state: *Overall agreement requires an octupole deformation of  $\beta_3 \approx 0.1$*  Our results in Table 2 agree very well with this analysis, both in terms of where the effect occurs ( $A \approx 219\text{--}229$ ) (also cf. Ref. [16]) and the magnitude of  $\beta_3$  ( $\approx 0.1$ ).

The first global nuclear-mass calculation in which octupole deformations were consistently taken into account was the nuclear-mass model/table FRLDM (1992) [1]. It led to a clear improvement in the calculated masses in the region near  $^{222}\text{Ra}$  as can be seen from comparing Fig. 1 in Ref. [29] with Fig. 1 in Ref. [1]. However, the effect of octupole shape degrees of freedom on nuclear masses was not quantified. In Ref. [10] we show that for the nuclei where we find an effect of reflection asymmetry the calculated masses are on the average too high by 1.032 MeV, when reflection asymmetry is not taken into account. When reflection asymmetry is taken into account the absolute value of the mean deviation  $\mu$  decreases to only 0.168 MeV.

As mentioned above we have performed a more accurate calculation of reflection asymmetry in the nuclear ground state. In the previous studies we only looked for octupole effects on the nuclear ground state if the minimum found in  $(\epsilon_2, \epsilon_4)$  space was unstable with respect to small deviations from reflection symmetry. This restriction was due to the computational limitations at the time. We have now established that sometimes a lower minimum is found for reflection asymmetric shapes for some nuclei even if the reflection-symmetric minimum is stable with respect to small octupole deformations. That is two minima exist, one reflection symmetric, and one reflection

asymmetric, and they are separated by a saddle. Another improvement in the current study is that the reflection-symmetric minimum is determined in a full 3D minimization in  $(\epsilon_2, \epsilon_4, \epsilon_6)$  space and the reflection-asymmetric minimum in a full 4D minimization in  $(\epsilon_2, \epsilon_3, \epsilon_4, \epsilon_6)$  space. The effect of the improvements is that we find that the region beyond Pb where we obtain reflection-asymmetric ground states extends slightly further in neutron number  $N$ . For example, for Th we find an effect for  $N = 136, 137$ , and  $138$ , whereas in the FRLDM (1992) table [1] the effect of the octupole degree of freedom only extends to  $N = 135$ . The situation is similar for other actinide isotope chains.

We are grateful to Arnold Sierk for many discussions during the course of this investigation and for a careful reading of the final manuscript. Comments by Henrik Uhrenholt<sup>2</sup> on the PNP and BCS pairing models are highly appreciated. This work was carried out under the auspices of the National Nuclear Security Administration of the U.S. Department of Energy at Los Alamos National Laboratory under Contract No. DE-AC52-06NA25396. This work was also supported by a travel grant to JUSTIPEN (Japan-U.S. Theory Institute for Physics with Exotic Nuclei) under grant number DE-FG02-06ER41407 (U. Tennessee).

## 5 APPENDIX

In our 1995 mass paper [1] and in a related paper [50] a number of misprints occurred. They have not migrated into any calculation. For completeness we give the corrected equations here. The equation numbers refer to the equation numbers in the original papers. Equation (20) in [1] should read

$$v = \cos 2\phi_t = \frac{\xi^2 - \eta^2}{\xi^2 + \eta^2} = \frac{\left[1 + \frac{1}{3}\epsilon_2 \cos \gamma\right] \cos 2\phi + \left(\frac{1}{3}\right)^{1/2} \epsilon_2 \sin \gamma}{1 + \frac{1}{3}\epsilon_2 \cos \gamma + \left(\frac{1}{3}\right)^{1/2} \epsilon_2 \sin \gamma \cos 2\phi}$$

This also applies to Eq. (33) in [50].

Equation (33) in [1] middle line should read

$$SY_{44} = \sqrt{\frac{315}{128\pi}} \sin^4 \theta \cos 4\phi = \sqrt{\frac{315}{128\pi}} (1 - u^2)^2 (2v^2 - 1)$$

This also applies to Eq. (A.10) in the appendix of Ref. [50], middle line.

A related equation in the Appendix of Ref. [50], Equation (A.17) third line is missing a factor 2 and should read

$$\frac{\partial SY_{44}}{\partial u} = -\sqrt{\frac{315}{128\pi}} 4u(1 - u^2)(2v^2 - 1)$$

---

<sup>2</sup>Uhrenholt was known as Olofsson before September 2, 2007

## References

- [1] P. Möller, J. R. Nix, W. D. Myers, and W. J. Swiatecki, *Atomic Data Nucl. Data Tables* **59** (1995) 185.
- [2] M. Bolsterli, E. O. Fiset, J. R. Nix, and J. L. Norton, *Phys. Rev. C* **5** (1972) 1050.
- [3] V. M. Strutinsky, *Nucl. Phys.* **A95** (1967) 420.
- [4] V. M. Strutinsky, *Nucl. Phys.* **A122** (1968) 1.
- [5] H. J. Lipkin, *Ann. Phys. (N. Y.)* **9** (1960) 272.
- [6] Y. Nogami, *Phys. Rev.* **134** (1964) B313.
- [7] H. C. Pradhan, Y. Nogami, and J. Law, *Nucl. Phys.* **A201** (1973) 357.
- [8] P. Möller and J. R. Nix, *Nucl. Phys.* **A536** (1992) 20.
- [9] P. Möller, A. J. Sierk, and A. Iwamoto, *Phys. Rev. Lett.* **67** (2004) 072501.
- [10] P. Möller, R. Bengtsson, P. Olivius, B. G. Carlsson, and T. Ichikawa, *Phys. Rev. Lett.* **97** (2006) 162502.
- [11] P. Möller, D. G. Madland, A. J. Sierk, and A. Iwamoto, *Nature* **409** (2001) 785.
- [12] P. Möller and J. R. Nix, *Nucl. Phys.* **A361** (1981) 117.
- [13] G. A. Leander, R. K. Sheline, P. Möller, P. Olanders, I. Ragnarsson, and A. J. Sierk, *Nucl. Phys.* **A388** (1982) 452.
- [14] G. A. Leander and Y. S. Chen, *Phys. Rev. C* **37** (1988) 2744.
- [15] S. Frauendorf, *Rev. Mod. Phys.* **73** (2001) 463.
- [16] P. A. Butler and W. Nazarewicz, *Rev. Mod. Phys.* **66** (1996) 349.
- [17] S. Åberg, H. Flocard, and W. Nazarewicz, *Ann. Rev. Nucl. Sci.* **40** (1990) 439.
- [18] J. Skalski, S. Mizutori, and W. Nazarewicz, *Nucl. Phys.* **A617** (1997) 282.
- [19] D. A. Arseniev, A. Sobiczewski, V. G. Soloviev, *Nucl. Phys.* **A126** (1969) 15.
- [20] S. G. Nilsson, C. F. Tsang, A. Sobiczewski, Z. Szymański, S. Wycech, C. Gustafson, I.-L. Lamm, P. Möller, and B. Nilsson, *Nucl. Phys.* **A131** (1969) 1.
- [21] P. Möller, *Nucl. Phys.* **A192** (1972) 529.
- [22] D. A. Arseniev, A. Sobiczewski, V. G. Soloviev, *Nucl. Phys.* **A126** (1969) 269.
- [23] U. Götz, H. C. Pauli, and K. Adler, *Nucl. Phys.* **A175** (1971) 481.
- [24] U. Götz, H. C. Pauli, and K. Junker, *Phys. Lett.* **39B** (1972) 436.
- [25] U. Götz, H. C. Pauli, K. Adler, and K. Junker, *Nucl. Phys.* **A192** (1972) 1.
- [26] P. Möller, S. G. Nilsson, and J. R. Nix, *Nucl. Phys.* **A229** (1974) 292.
- [27] P. Möller and J. R. Nix, *Atomic Data Nucl. Data Tables* **26** (1981) 165.
- [28] P. Möller and J. R. Nix, *Atomic Data Nucl. Data Tables* **39** (1988) 213.

- [29] P. Möller, W. D. Myers, W. J. Swiatecki, and J. Treiner, *Atomic Data Nucl. Data Tables* **39** (1988) 225.
- [30] S. E. Larsson, *Phys. Scr.* **8** (1973) 17.
- [31] A. Faessler, J. E. Galonska, U. Götz, and H. C. Pauli, *Nucl Phys* **A230** (1974) 302.
- [32] H. Olofsson, R. Bengtsson, and P. Möller, *Nucl. Phys.* **A784** (2007) 104.
- [33] F. K. McGowan, R. L. Robinson, P. H. Stelson, and W. T. Milner, *Nucl. Phys.* **A113** (1969) 529.
- [34] N. Kaffrell, N. Trautmann, and G. Hermann, *Phys. Rev. C* **8** (1973) 320.
- [35] J. Äystö, P. P. Jauho, Z. Janas, A. Jokinen, J. M. Parmonen, H. Penttilä, P. Taskinen, R. Béraud, R. Duffait, A. Emsalem, J. Meyer, M. Meyer, N. Redon, M. E. Leino, K. Eskola, P. Dendooven, *Nucl Phys.* **A515** (1990) 365.
- [36] J. A. Shannon, W. R. Phillips, J. L. Durell, B. J. Varley, W. Urban, C. J. Pearson, I. Ahmad, C. J. Lister, L. R. Morss, K. L. Nash, C. W. Williams, N. Schulz, E. Lubkiewicz, M. Bentaleb, *Phys. Lett. B* **22** (1994) 136.
- [37] S.J. Zhu, Y.X. Luo, J.H. Hamilton, A. V. Ramayya, X.L. Che, Z. Jiang, J.K. Hwang, J.L. Wood, M.A. Stoyer, R. Donangelo, J.D. Cole, C. Goodin, and J.O. Rasmussen, *Euro. Phys Journ. A*, to be published (2007).
- [38] I. Ragnarsson, A. Sobiczewski, R. K. Sheline, S. E. Larsson, and B. Nerlo-Pomorska, *Nucl. Phys.* **A233** (1974) 329.
- [39] M. Girod and B. Grammaticos, *Phys. Rev. Lett.* **40** (1978) 361.
- [40] M. Girod and B. Grammaticos, *Phys. Rev. C* **27** (1983) 2317.
- [41] N. Redon, J. Meyer, M. Meyer, P. Quentin, P. Bonche, H. Flocard, P. H. Heenen, *Phys. Rev. C* **38** (1988) 550.
- [42] B. D. Kern, R. L. Mlekodaj, G. A. Leander, M. O. Kortelahti, E. F. Zganjar, R. A. Braga, R. W. Fink, C. P. Perez, W. Nazarewicz, P. B. Semmes *Phys. Rev. C* **36** (1987) 1514.
- [43] A. K. Dutta, J. M. Pearson, and F. Tondeur, *Phys. Rev. C* **61** (2000) 054303.
- [44] Y. Aboussir, J. M. Pearson, A. K. Dutta, and F. Tondeur, *Atomic Data Nucl. Data Tables* **61** (1995) 127.
- [45] P. Vogel, *Nucl. Phys.* **A112** (1968) 583.
- [46] P. Möller, S. G. Nilsson, and R. K. Sheline, *Phys. Lett.* **40B** (1972) 329.
- [47] K. Neergård and P. Vogel, *Nucl. Phys.* **A145** (1970) 33.
- [48] K. Neergård and P. Vogel, *Nucl. Phys.* **A149** (1970) 217.
- [49] W. Nazarewicz, P. Olanders, I. Ragnarsson, J. Dudek, G. A. Leander, P. Möller, and E. Ruchowska, *Nucl. Phys.* **A429** (1984) 269.
- [50] P. Möller and A. Iwamoto, *Nucl. Phys.* **A575** (1994) 381.

### EXPLANATION OF TABLE 1

**Table 1 Calculated Effect of Axial Asymmetry on Nuclear Ground-State Masses and Deformations**

<b>Z</b>	Proton number. The table is ordered by increasing proton number. The corresponding chemical symbol of each named element is given in parentheses.
<b>N</b>	Neutron number.
<b>A</b>	Mass Number.
$\epsilon_2$	Calculated ground-state quadrupole deformation in the Nilsson perturbed-spheroid parameterization.
$\epsilon_4$	Calculated ground-state hexadecapole deformation in the Nilsson perturbed-spheroid parameterization.
$\gamma$	Calculated ground-state gamma deformation in the Nilsson perturbed-spheroid parameterization.
$\Delta E_\gamma$	Calculated decrease in potential energy due to triaxiality. We only present nuclei for which the calculated decrease in energy due to triaxiality is equal to or larger than 0.01 MeV.

Table 1: Calculated Effect of Axial Asymmetry on Nuclear Ground-State Masses and Deformations

$N$	$A$	$\epsilon_2$	$\epsilon_4$	$\gamma$	$\Delta E_\gamma$ (MeV)	$N$	$A$	$\epsilon_2$	$\epsilon_4$	$\gamma$	$\Delta E_\gamma$ (MeV)	$N$	$A$	$\epsilon_2$	$\epsilon_4$	$\gamma$	$\Delta E_\gamma$ (MeV)										
<b><math>Z = 9</math> (F)</b>																											
27	36	0.225	-0.12	40.0	0.03	27	45	0.100	0.02	30.0	0.03	41	72	0.200	0.02	40.0	0.08										
<b><math>Z = 11</math> (Na)</b>																											
31	42	0.275	0.04	32.5	0.21	49	67	0.100	0.02	32.5	0.06	43	74	0.125	-0.02	12.5	0.01										
<b><math>Z = 12</math> (Mg)</b>																											
30	42	0.275	0.06	32.5	0.03	27	46	0.075	0.00	27.5	0.01	52	83	0.125	-0.02	20.0	0.03										
31	43	0.275	0.04	32.5	0.29	45	64	0.125	-0.02	10.0	0.02	53	84	0.125	-0.02	15.0	0.05										
32	44	0.225	0.04	30.0	0.11	46	65	0.125	0.00	12.5	0.02	54	85	0.150	-0.02	15.0	0.09										
35	47	0.225	0.04	30.0	0.30	47	66	0.125	0.02	15.0	0.02	55	86	0.175	0.00	15.0	0.05										
<b><math>Z = 13</math> (Al)</b>																											
26	39	0.275	-0.08	37.5	0.04	49	68	0.100	0.00	37.5	0.02	60	91	0.225	0.02	20.0	0.11										
27	40	0.300	-0.10	47.5	0.15	<b><math>Z = 24</math> (Cr)</b>																					
28	41	0.325	-0.12	57.5	0.02	18	42	0.150	0.02	32.5	0.03	64	95	0.275	0.02	17.5	0.22										
29	42	0.275	-0.10	55.0	0.03	<b><math>Z = 25</math> (Mn)</b>																					
30	43	0.275	-0.06	55.0	0.03	18	43	0.200	0.02	32.5	0.04	66	97	0.275	0.02	17.5	0.19										
31	44	0.250	0.00	50.0	0.14	63	88	0.300	-0.02	7.5	0.04	67	98	0.275	0.04	10.0	0.08										
32	45	0.125	0.00	32.5	0.07	64	89	0.300	-0.02	7.5	0.02	73	104	0.225	0.04	22.5	0.17										
33	46	0.125	0.02	32.5	0.02	<b><math>Z = 26</math> (Fe)</b>																					
35	48	0.175	0.02	30.0	0.07	17	43	0.225	0.06	32.5	0.08	75	106	0.200	0.04	30.0	0.38										
36	49	0.175	0.02	30.0	0.04	19	45	0.100	0.00	30.0	0.02	<b><math>Z = 32</math> (Ge)</b>															
<b><math>Z = 14</math> (Si)</b>																											
26	40	0.275	-0.08	42.5	0.03	17	44	0.250	0.02	47.5	0.05	32	64	0.225	0.02	32.5	0.07										
33	47	0.125	0.00	40.0	0.04	18	45	0.250	0.02	52.5	0.01	37	69	0.225	0.04	42.5	0.07										
<b><math>Z = 15</math> (P)</b>																											
27	42	0.275	-0.06	50.0	0.08	37	64	0.100	0.02	42.5	0.04	41	73	0.225	0.04	42.5	0.07										
30	45	0.250	0.00	55.0	0.03	41	68	0.050	0.00	27.5	0.02	42	74	0.225	0.04	40.0	0.18										
31	46	0.125	0.02	35.0	0.05	56	83	0.050	0.00	22.5	0.02	43	75	0.250	0.04	35.0	0.38										
32	47	0.125	0.02	32.5	0.02	59	86	0.050	0.00	22.5	0.02	60	92	0.225	0.02	20.0	0.07										
35	50	0.175	0.04	42.5	0.03	67	94	0.300	0.04	2.5	0.02	63	95	0.275	0.02	20.0	0.09										
<b><math>Z = 16</math> (S)</b>																											
16	32	0.250	0.12	32.5	0.01	27	55	0.025	0.00	35.0	0.02	65	97	0.300	0.02	20.0	0.25										
17	33	0.250	0.10	45.0	0.03	<b><math>Z = 29</math> (Cu)</b>																					
29	45	0.250	0.00	57.5	0.01	35	64	0.125	0.02	17.5	0.02	67	99	0.275	0.04	10.0	0.04										
31	47	0.225	0.06	50.0	0.13	57	86	0.100	-0.02	32.5	0.17	73	105	0.225	0.06	22.5	0.15										
41	57	0.350	0.08	30.0	0.22	59	88	0.100	-0.02	32.5	0.20	74	106	0.200	0.04	27.5	0.35										
42	58	0.350	0.08	30.0	0.31	65	94	0.300	0.02	10.0	0.05	75	107	0.200	0.04	30.0	0.40										
43	59	0.325	0.08	30.0	0.19	<b><math>Z = 30</math> (Zn)</b>																					
<b><math>Z = 17</math> (Cl)</b>																											
26	43	0.175	0.04	15.0	0.03	64	94	0.300	0.02	12.5	0.02	<b><math>Z = 33</math> (As)</b>															
27	44	0.250	0.02	47.5	0.02	65	95	0.300	0.02	12.5	0.09	43	76	0.250	0.04	45.0	0.04										
29	46	0.200	0.04	55.0	0.02	73	103	0.225	0.04	22.5	0.11	51	84	0.125	0.02	7.5	0.03										
30	47	0.200	0.06	52.5	0.04	74	104	0.200	0.02	25.0	0.25	61	94	0.300	-0.04	7.5	0.03										
31	48	0.225	0.08	55.0	0.08	75	105	0.200	0.04	30.0	0.13	62	95	0.300	-0.02	10.0	0.03										
32	49	0.175	0.08	55.0	0.03	<b><math>Z = 31</math> (Ga)</b>																					
33	50	0.175	0.06	45.0	0.09	30	61	0.150	-0.02	10.0	0.03	64	97	0.300	0.00	20.0	0.25										
37	54	0.225	0.10	55.0	0.02	31	62	0.200	0.00	32.5	0.05	65	98	0.300	0.02	20.0	0.25										
42	59	0.250	0.10	55.0	0.01	32	63	0.200	0.02	32.5	0.06	66	99	0.300	0.02	22.5	0.11										
43	60	0.275	0.06	30.0	0.36	36	67	0.175	0.02	32.5	0.03	67	100	0.275	0.06	7.5	0.02										
44	61	0.275	0.06	30.0	0.09	37	68	0.175	0.02	45.0	0.03	73	106	0.200	0.06	7.5	0.03										
46	63	0.175	0.02	10.0	0.03	38	69	0.175	0.02	45.0	0.02	74	107	0.200	0.06	22.5	0.15										

Table 1: Continued. Calculated Effect of Triaxiality on Ground-State Masses and Deformations

$N$	$A$	$\epsilon_2$	$\epsilon_4$	$\gamma$	$\Delta E_\gamma$ (MeV)	$N$	$A$	$\epsilon_2$	$\epsilon_4$	$\gamma$	$\Delta E_\gamma$ (MeV)	$N$	$A$	$\epsilon_2$	$\epsilon_4$	$\gamma$	$\Delta E_\gamma$ (MeV)										
<b><math>Z = 33</math> (As)</b>																											
75	108	0.200	0.06	25.0	0.26	31	70	0.275	0.02	5.0	0.01	68	111	0.275	0.06	15.0	0.04										
76	109	0.175	0.06	25.0	0.05	55	94	0.200	0.00	42.5	0.08	72	115	0.225	0.06	52.5	0.02										
77	110	0.150	0.04	20.0	0.06	<b><math>Z = 40</math> (Zr)</b>																					
<b><math>Z = 34</math> (Se)</b>																											
63	97	0.325	0.00	17.5	0.12	32	72	0.275	0.04	35.0	0.27	74	117	0.200	0.06	42.5	0.26										
64	98	0.325	0.00	20.0	0.21	55	95	0.175	0.00	37.5	0.12	75	118	0.200	0.06	40.0	0.23										
65	99	0.325	0.02	20.0	0.27	74	114	0.175	0.06	57.5	0.08	76	119	0.175	0.06	45.0	0.10										
66	100	0.325	0.02	20.0	0.03	54	95	0.175	0.00	35.0	0.09	89	132	0.125	-0.04	5.0	0.02										
73	107	0.225	0.08	12.5	0.02	55	96	0.200	0.00	37.5	0.19	95	138	0.250	-0.04	12.5	0.12										
74	108	0.200	0.06	17.5	0.04	56	97	0.200	0.00	30.0	0.12	96	139	0.250	-0.02	12.5	0.11										
75	109	0.200	0.06	25.0	0.18	57	98	0.225	0.02	22.5	0.04	97	140	0.275	-0.02	15.0	0.12										
76	110	0.175	0.06	22.5	0.13	65	106	0.325	0.04	15.0	0.15	98	141	0.275	0.00	15.0	0.11										
77	111	0.150	0.06	20.0	0.03	66	107	0.325	0.06	15.0	0.16	99	142	0.275	0.00	7.5	0.02										
<b><math>Z = 35</math> (Br)</b>																											
63	98	0.325	0.00	15.0	0.07	67	108	0.300	0.06	7.5	0.02	37	81	0.250	0.06	47.5	0.05										
64	99	0.325	0.00	17.5	0.14	73	114	0.200	0.06	50.0	0.03	38	82	0.225	0.08	52.5	0.01										
65	100	0.325	0.02	17.5	0.19	96	137	0.275	-0.02	7.5	0.01	44	88	0.250	0.06	37.5	0.03										
<b><math>Z = 42</math> (Mo)</b>																											
73	108	0.225	0.06	7.5	0.04	35	77	0.275	0.06	57.5	0.03	57	101	0.200	0.02	22.5	0.11										
74	109	0.200	0.06	30.0	0.10	54	96	0.175	0.00	32.5	0.09	58	102	0.225	0.04	27.5	0.18										
75	110	0.200	0.06	30.0	0.39	55	97	0.200	0.00	32.5	0.12	59	103	0.225	0.04	27.5	0.32										
76	111	0.175	0.06	30.0	0.26	56	98	0.200	0.00	27.5	0.16	60	104	0.250	0.04	27.5	0.38										
77	112	0.150	0.06	32.5	0.21	57	99	0.225	0.02	27.5	0.27	61	105	0.250	0.04	27.5	0.35										
<b><math>Z = 36</math> (Kr)</b>																											
52	88	0.075	0.00	52.5	0.08	58	100	0.225	0.02	25.0	0.15	62	106	0.250	0.04	27.5	0.41										
64	100	0.325	0.02	10.0	0.03	63	105	0.300	0.02	17.5	0.11	63	107	0.275	0.04	25.0	0.57										
65	101	0.325	0.02	12.5	0.07	64	106	0.300	0.02	17.5	0.26	64	108	0.275	0.04	25.0	0.63										
74	110	0.200	0.06	27.5	0.15	65	107	0.325	0.04	20.0	0.30	65	109	0.275	0.04	22.5	0.67										
75	111	0.200	0.06	30.0	0.27	66	108	0.300	0.04	17.5	0.30	66	110	0.275	0.04	22.5	0.47										
76	112	0.150	0.06	35.0	0.13	67	109	0.300	0.06	15.0	0.04	67	111	0.275	0.04	25.0	0.22										
77	113	0.150	0.06	37.5	0.11	73	115	0.200	0.06	50.0	0.06	72	116	0.225	0.06	45.0	0.07										
78	114	0.100	0.02	2.5	0.03	74	116	0.200	0.06	42.5	0.10	73	117	0.225	0.06	42.5	0.27										
<b><math>Z = 37</math> (Rb)</b>																											
31	68	0.250	0.02	47.5	0.08	96	138	0.250	-0.04	12.5	0.08	75	119	0.200	0.06	40.0	0.35										
32	69	0.275	0.04	50.0	0.07	97	139	0.275	-0.02	15.0	0.11	76	120	0.150	0.06	50.0	0.02										
33	70	0.275	0.04	55.0	0.03	<b><math>Z = 43</math> (Tc)</b>																					
43	80	0.250	0.06	55.0	0.02	54	97	0.175	-0.02	22.5	0.02	97	141	0.250	-0.02	15.0	0.16										
44	81	0.250	0.06	52.5	0.04	55	98	0.175	0.00	20.0	0.06	98	142	0.250	-0.02	15.0	0.12										
52	89	0.075	0.00	47.5	0.02	56	99	0.200	0.00	27.5	0.12	99	143	0.275	0.00	12.5	0.05										
54	91	0.150	0.00	42.5	0.01	57	100	0.225	0.02	30.0	0.26	104	148	0.275	0.04	12.5	0.03										
74	111	0.200	0.06	30.0	0.18	58	101	0.225	0.02	27.5	0.27	105	149	0.275	0.04	17.5	0.21										
75	112	0.200	0.06	30.0	0.06	59	102	0.225	0.02	27.5	0.26	106	150	0.275	0.04	32.5	0.31										
76	113	0.150	0.06	45.0	0.06	60	103	0.275	0.02	25.0	0.20	<b><math>Z = 45</math> (Rh)</b>															
77	114	0.150	0.06	45.0	0.05	61	104	0.275	0.02	25.0	0.20	38	83	0.250	0.08	45.0	0.05										
89	126	0.100	0.00	30.0	0.11	62	105	0.275	0.02	22.5	0.31	39	84	0.250	0.08	45.0	0.04										
90	127	0.100	0.00	30.0	0.02	63	106	0.300	0.02	20.0	0.42	41	86	0.225	0.08	50.0	0.03										
<b><math>Z = 38</math> (Sr)</b>																											
31	69	0.275	0.04	40.0	0.04	64	107	0.300	0.04	22.5	0.52	43	88	0.250	0.06	40.0	0.05										
32	70	0.275	0.04	40.0	0.12	65	108	0.300	0.04	22.5	0.59	44	89	0.250	0.06	37.5	0.08										
43	81	0.325	0.04	12.5	0.07	66	109	0.300	0.04	20.0	0.49	59	104	0.225	0.04	27.5	0.17										

Table 1: Continued. Calculated Effect of Triaxiality on Ground-State Masses and Deformations

$N$	$A$	$\epsilon_2$	$\epsilon_4$	$\gamma$	$\Delta E_\gamma$ (MeV)	$N$	$A$	$\epsilon_2$	$\epsilon_4$	$\gamma$	$\Delta E_\gamma$ (MeV)	$N$	$A$	$\epsilon_2$	$\epsilon_4$	$\gamma$	$\Delta E_\gamma$ (MeV)										
<b><math>Z = 45</math> (Rh)</b>																											
61	106	0.250	0.04	30.0	0.44	105	152	0.250	0.04	7.5	0.02	116	169	0.150	0.02	40.0	0.09										
62	107	0.250	0.04	27.5	0.51	106	153	0.250	0.04	12.5	0.05	119	172	0.100	0.04	15.0	0.01										
63	108	0.250	0.04	27.5	0.56	107	154	0.250	0.06	15.0	0.07	120	173	0.100	0.02	30.0	0.09										
64	109	0.275	0.04	25.0	0.65	108	155	0.225	0.06	7.5	0.04	121	174	0.075	0.02	30.0	0.13										
65	110	0.275	0.04	25.0	0.62	<b><math>Z = 48</math> (Cd)</b>																					
66	111	0.275	0.04	25.0	0.33	73	121	0.125	0.02	20.0	0.01	53	107	0.125	-0.06	7.5	0.01										
67	112	0.275	0.04	27.5	0.11	<b><math>Z = 49</math> (In)</b>																					
72	117	0.225	0.06	45.0	0.10	65	114	0.100	0.00	47.5	0.02	64	118	0.225	-0.02	10.0	0.04										
73	118	0.225	0.06	40.0	0.31	68	117	0.100	0.00	47.5	0.01	65	119	0.225	0.00	7.5	0.01										
74	119	0.200	0.06	35.0	0.36	69	118	0.100	0.02	47.5	0.02	73	127	0.175	0.00	22.5	0.05										
75	120	0.200	0.06	35.0	0.37	70	119	0.100	0.02	45.0	0.04	74	128	0.175	0.00	25.0	0.05										
76	121	0.175	0.06	40.0	0.16	71	120	0.100	0.02	42.5	0.04	75	129	0.175	0.02	27.5	0.14										
77	122	0.150	0.06	45.0	0.01	72	121	0.100	0.02	40.0	0.05	76	130	0.150	0.02	30.0	0.13										
95	140	0.225	-0.04	7.5	0.01	73	122	0.100	0.02	32.5	0.07	79	133	0.050	0.00	42.5	0.04										
96	141	0.250	-0.02	12.5	0.03	75	124	0.100	0.04	47.5	0.01	120	174	0.100	0.02	30.0	0.08										
97	142	0.250	-0.02	12.5	0.11	<b><math>Z = 50</math> (Sn)</b>																					
98	143	0.275	-0.02	15.0	0.08	119	169	0.100	0.04	25.0	0.07	<b><math>Z = 55</math> (Cs)</b>															
99	144	0.275	0.00	12.5	0.06	<b><math>Z = 51</math> (Sb)</b>																					
100	145	0.275	0.00	12.5	0.02	114	165	0.150	0.02	40.0	0.04	64	119	0.250	-0.02	15.0	0.08										
104	149	0.275	0.04	15.0	0.06	116	167	0.100	0.02	30.0	0.01	65	120	0.250	0.00	12.5	0.03										
105	150	0.275	0.04	32.5	0.05	118	169	0.100	0.02	30.0	0.07	74	129	0.175	0.02	17.5	0.05										
106	151	0.250	0.06	15.0	0.25	119	170	0.100	0.02	30.0	0.13	75	130	0.175	0.02	22.5	0.19										
107	152	0.250	0.06	17.5	0.37	120	171	0.075	0.02	30.0	0.14	76	131	0.150	0.02	27.5	0.18										
108	153	0.250	0.06	17.5	0.38	<b><math>Z = 52</math> (Te)</b>																					
<b><math>Z = 46</math> (Pd)</b>																	73	125	0.125	0.02	47.5	0.05					
43	89	0.250	0.08	45.0	0.04	114	166	0.150	0.02	30.0	0.12	98	153	0.225	-0.04	2.5	0.04										
61	107	0.225	0.04	27.5	0.11	115	167	0.150	0.02	35.0	0.12	120	175	0.100	0.04	12.5	0.02										
62	108	0.225	0.04	27.5	0.24	119	171	0.100	0.04	15.0	0.03	121	176	0.100	0.04	30.0	0.11										
63	109	0.250	0.04	27.5	0.31	120	172	0.075	0.02	25.0	0.07	122	177	0.075	0.02	30.0	0.04										
64	110	0.250	0.04	27.5	0.32	<b><math>Z = 53</math> (I)</b>																					
65	111	0.275	0.04	25.0	0.27	53	106	0.125	-0.06	12.5	0.03	57	113	0.225	-0.08	7.5	0.01										
72	118	0.225	0.06	47.5	0.04	54	107	0.125	-0.06	10.0	0.03	64	120	0.275	-0.02	15.0	0.07										
73	119	0.225	0.06	42.5	0.20	56	109	0.150	-0.04	10.0	0.02	65	121	0.275	-0.02	15.0	0.03										
74	120	0.200	0.06	37.5	0.22	57	110	0.150	-0.04	10.0	0.05	75	131	0.175	0.02	20.0	0.09										
75	121	0.175	0.06	30.0	0.20	59	112	0.175	-0.02	5.0	0.01	76	132	0.150	0.02	20.0	0.11										
76	122	0.150	0.06	37.5	0.07	62	115	0.200	-0.02	10.0	0.04	77	133	0.150	0.02	25.0	0.17										
97	143	0.250	-0.02	12.5	0.08	63	116	0.200	-0.02	10.0	0.05	78	134	0.125	0.02	30.0	0.12										
98	144	0.250	-0.02	12.5	0.05	64	117	0.200	-0.02	10.0	0.07	79	135	0.100	0.02	32.5	0.12										
104	150	0.275	0.04	15.0	0.03	65	118	0.225	0.00	10.0	0.06	120	176	0.100	0.04	12.5	0.01										
105	151	0.250	0.04	10.0	0.08	66	119	0.225	0.00	10.0	0.05	121	177	0.100	0.04	30.0	0.17										
106	152	0.250	0.06	15.0	0.19	72	125	0.175	0.00	30.0	0.08	122	178	0.075	0.02	30.0	0.08										
107	153	0.250	0.06	17.5	0.29	73	126	0.150	0.00	25.0	0.12	<b><math>Z = 57</math> (La)</b>															
108	154	0.250	0.06	17.5	0.24	74	127	0.150	0.00	27.5	0.10	63	120	0.275	-0.04	5.0	0.02										
109	155	0.250	0.08	20.0	0.24	75	128	0.150	0.02	30.0	0.11	64	121	0.275	-0.02	10.0	0.07										
110	156	0.225	0.08	17.5	0.16	79	132	0.050	0.00	42.5	0.04	65	122	0.275	-0.02	10.0	0.12										
<b><math>Z = 47</math> (Ag)</b>																	89	142	0.125	-0.04	7.5	0.04					
73	120	0.175	0.04	30.0	0.09	93	146	0.150	-0.06	7.5	0.07	74	131	0.200	0.02	17.5	0.11										
74	121	0.175	0.06	30.0	0.05	114	167	0.175	0.02	35.0	0.04	75	132	0.175	0.02	25.0	0.13										
75	122	0.150	0.04	30.0	0.09	115	168	0.175	0.02	40.0	0.05	76	133	0.175	0.02	25.0	0.24										

Table 1: Continued. Calculated Effect of Triaxiality on Ground-State Masses and Deformations

$N$	$A$	$\epsilon_2$	$\epsilon_4$	$\gamma$	$\Delta E_\gamma$ (MeV)	$N$	$A$	$\epsilon_2$	$\epsilon_4$	$\gamma$	$\Delta E_\gamma$ (MeV)	$N$	$A$	$\epsilon_2$	$\epsilon_4$	$\gamma$	$\Delta E_\gamma$ (MeV)										
<b><math>Z = 57</math> (La)</b>																											
77	134	0.150	0.02	25.0	0.24	75	138	0.225	0.04	22.5	0.23	123	194	0.100	0.02	57.5	0.01										
78	135	0.125	0.02	27.5	0.14	76	139	0.200	0.04	22.5	0.30	129	200	0.025	0.00	30.0	0.02										
79	136	0.100	0.02	32.5	0.06	77	140	0.200	0.04	25.0	0.52	<b><math>Z = 72</math> (Hf)</b>															
121	178	0.100	0.04	30.0	0.17	78	141	0.175	0.04	30.0	0.52	77	149	0.175	0.06	17.5	0.10										
122	179	0.100	0.02	30.0	0.13	79	142	0.175	0.04	37.5	0.18	79	151	0.150	0.04	52.5	0.02										
<b><math>Z = 58</math> (Ce)</b>																											
75	133	0.175	0.04	15.0	0.06	<b><math>Z = 64</math> (Gd)</b>																					
76	134	0.175	0.04	22.5	0.24	65	129	0.325	0.02	15.0	0.03	78	151	0.175	0.04	45.0	0.04										
77	135	0.175	0.04	25.0	0.21	66	130	0.325	0.04	15.0	0.01	79	152	0.150	0.04	47.5	0.05										
78	136	0.150	0.02	27.5	0.14	75	139	0.225	0.04	20.0	0.16	<b><math>Z = 74</math> (W)</b>															
79	137	0.125	0.02	22.5	0.14	76	140	0.200	0.04	20.0	0.25	84	158	0.075	0.00	10.0	0.04										
80	138	0.050	0.00	15.0	0.01	77	141	0.200	0.04	25.0	0.48	<b><math>Z = 75</math> (Re)</b>															
121	179	0.100	0.04	27.5	0.15	78	142	0.175	0.04	30.0	0.37	83	158	0.050	0.00	22.5	0.01										
122	180	0.100	0.02	30.0	0.15	79	143	0.175	0.04	42.5	0.06	123	198	0.075	0.02	50.0	0.02										
<b><math>Z = 59</math> (Pr)</b>																											
75	134	0.200	0.04	22.5	0.19	119	183	0.175	0.02	57.5	0.01	<b><math>Z = 77</math> (Ir)</b>															
76	135	0.175	0.04	22.5	0.22	<b><math>Z = 65</math> (Tb)</b>																					
77	136	0.175	0.04	25.0	0.30	65	130	0.325	0.04	17.5	0.16	115	192	0.150	0.06	17.5	0.06										
78	137	0.150	0.04	30.0	0.23	66	131	0.300	0.04	12.5	0.16	<b><math>Z = 78</math> (Pt)</b>															
79	138	0.125	0.02	17.5	0.12	67	132	0.300	0.04	10.0	0.08	89	167	0.125	0.00	30.0	0.01										
121	180	0.100	0.04	27.5	0.12	75	140	0.225	0.04	17.5	0.14	90	168	0.125	0.00	22.5	0.05										
122	181	0.100	0.02	30.0	0.13	76	141	0.225	0.04	22.5	0.27	91	169	0.125	0.00	20.0	0.03										
<b><math>Z = 60</math> (Nd)</b>																											
75	135	0.200	0.04	20.0	0.15	77	142	0.200	0.04	22.5	0.45	92	170	0.125	0.00	17.5	0.02										
76	136	0.200	0.04	25.0	0.29	78	143	0.200	0.04	25.0	0.31	93	171	0.125	0.00	15.0	0.05										
77	137	0.175	0.04	25.0	0.38	<b><math>Z = 66</math> (Dy)</b>																					
78	138	0.150	0.04	30.0	0.33	67	133	0.300	0.06	10.0	0.08	96	174	0.150	0.02	20.0	0.10										
79	139	0.150	0.04	40.0	0.16	75	141	0.225	0.06	15.0	0.06	97	175	0.150	0.02	20.0	0.10										
121	181	0.100	0.04	25.0	0.05	76	142	0.225	0.06	20.0	0.19	109	187	0.175	0.06	7.5	0.03										
122	182	0.100	0.02	30.0	0.13	77	143	0.200	0.04	20.0	0.33	110	188	0.175	0.06	10.0	0.02										
<b><math>Z = 61</math> (Pm)</b>																											
74	135	0.225	0.04	17.5	0.03	78	144	0.200	0.04	25.0	0.08	111	189	0.175	0.06	15.0	0.08										
75	136	0.200	0.04	20.0	0.17	79	145	0.175	0.04	52.5	0.03	112	190	0.150	0.04	25.0	0.23										
76	137	0.200	0.04	25.0	0.38	<b><math>Z = 67</math> (Ho)</b>																					
77	138	0.175	0.04	25.0	0.45	76	143	0.225	0.06	17.5	0.15	114	192	0.150	0.04	30.0	0.30										
78	139	0.175	0.04	30.0	0.44	77	144	0.225	0.06	20.0	0.21	115	193	0.150	0.04	30.0	0.21										
79	140	0.150	0.04	35.0	0.27	78	145	0.200	0.04	22.5	0.05	116	194	0.125	0.04	27.5	0.15										
119	180	0.150	0.04	17.5	0.06	79	146	0.175	0.04	52.5	0.01	117	195	0.125	0.04	27.5	0.21										
122	183	0.100	0.02	30.0	0.10	85	152	0.125	-0.04	10.0	0.02	<b><math>Z = 79</math> (Au)</b>															
<b><math>Z = 62</math> (Sm)</b>																											
74	136	0.225	0.04	17.5	0.07	77	145	0.200	0.06	12.5	0.13	90	169	0.100	0.02	52.5	0.02										
75	137	0.225	0.04	22.5	0.14	119	187	0.200	0.04	57.5	0.01	92	171	0.100	0.02	35.0	0.05										
76	138	0.200	0.04	22.5	0.33	<b><math>Z = 69</math> (Tm)</b>																					
77	139	0.200	0.04	27.5	0.48	77	146	0.200	0.06	10.0	0.07	94	173	0.125	0.02	32.5	0.27										
78	140	0.175	0.04	30.0	0.49	<b><math>Z = 70</math> (Yb)</b>																					
79	141	0.150	0.04	40.0	0.19	77	147	0.200	0.08	7.5	0.05	95	174	0.125	0.02	32.5	0.23										
119	181	0.150	0.06	15.0	0.02	<b><math>Z = 71</math> (Lu)</b>																					
122	184	0.100	0.02	30.0	0.02	77	148	0.200	0.08	7.5	0.05	96	175	0.125	0.02	30.0	0.25										
<b><math>Z = 63</math> (Eu)</b>																											
66	129	0.300	0.02	10.0	0.03	79	150	0.175	0.04	55.0	0.01	100	179	0.150	0.02	30.0	0.29										

Table 1: Continued. Calculated Effect of Triaxiality on Ground-State Masses and Deformations

$N$	$A$	$\epsilon_2$	$\epsilon_4$	$\gamma$	$\Delta E_\gamma$ (MeV)	$N$	$A$	$\epsilon_2$	$\epsilon_4$	$\gamma$	$\Delta E_\gamma$ (MeV)	$N$	$A$	$\epsilon_2$	$\epsilon_4$	$\gamma$	$\Delta E_\gamma$ (MeV)										
<b><math>Z = 79</math> (Au)</b>																											
101	180	0.150	0.02	27.5	0.10	159	243	0.200	0.04	15.0	0.04	107	196	0.250	0.02	15.0	0.10										
102	181	0.150	0.02	27.5	0.15	<b><math>Z = 85</math> (At)</b>																					
104	183	0.175	0.04	17.5	0.08	114	199	0.100	0.00	20.0	0.02	109	198	0.250	0.04	17.5	0.09										
106	185	0.175	0.04	12.5	0.04	115	200	0.100	0.00	22.5	0.02	110	199	0.250	0.00	45.0	0.12										
107	186	0.175	0.04	10.0	0.03	116	201	0.075	0.00	30.0	0.03	111	200	0.250	0.00	47.5	0.27										
108	187	0.175	0.04	17.5	0.05	143	228	0.175	-0.06	7.5	0.02	112	201	0.225	0.00	42.5	0.26										
109	188	0.150	0.04	17.5	0.13	155	240	0.225	0.02	12.5	0.07	113	202	0.225	0.02	42.5	0.35										
110	189	0.150	0.04	27.5	0.12	156	241	0.200	0.02	15.0	0.14	114	203	0.225	0.02	42.5	0.28										
111	190	0.150	0.04	27.5	0.21	157	242	0.200	0.02	17.5	0.15	115	204	0.225	0.04	45.0	0.21										
112	191	0.125	0.04	30.0	0.23	158	243	0.200	0.02	20.0	0.10	116	205	0.200	0.02	45.0	0.08										
113	192	0.125	0.04	30.0	0.34	159	244	0.200	0.02	22.5	0.05	117	206	0.200	0.04	52.5	0.04										
114	193	0.125	0.04	30.0	0.29	<b><math>Z = 86</math> (Rn)</b>																					
115	194	0.125	0.04	30.0	0.26	107	193	0.250	0.02	15.0	0.12	156	245	0.225	0.02	15.0	0.17										
116	195	0.125	0.04	30.0	0.09	116	202	0.100	0.00	30.0	0.04	157	246	0.225	0.02	17.5	0.31										
117	196	0.125	0.02	47.5	0.03	117	203	0.100	0.00	30.0	0.02	158	247	0.225	0.02	20.0	0.24										
137	216	0.100	-0.02	12.5	0.04	154	240	0.225	0.00	10.0	0.04	159	248	0.225	0.02	22.5	0.15										
<b><math>Z = 80</math> (Hg)</b>																											
96	176	0.125	0.02	40.0	0.06	156	242	0.225	0.02	15.0	0.12	<b><math>Z = 90</math> (Th)</b>															
97	177	0.125	0.02	40.0	0.13	157	243	0.200	0.02	15.0	0.16	108	198	0.250	0.02	15.0	0.26										
98	178	0.125	0.02	40.0	0.07	158	244	0.200	0.02	17.5	0.14	109	199	0.250	0.04	17.5	0.20										
99	179	0.125	0.02	42.5	0.07	159	245	0.200	0.02	20.0	0.08	110	200	0.250	0.04	20.0	0.09										
<b><math>Z = 81</math> (Tl)</b>																											
92	173	0.050	0.00	30.0	0.02	<b><math>Z = 87</math> (Fr)</b>																					
97	178	0.050	0.00	12.5	0.02	111	198	0.225	0.00	55.0	0.01	113	203	0.225	0.02	37.5	0.38										
99	180	0.050	0.00	30.0	0.04	115	202	0.200	0.02	52.5	0.02	114	204	0.225	0.02	40.0	0.40										
158	239	0.175	0.04	12.5	0.05	117	204	0.125	0.00	50.0	0.04	115	205	0.225	0.04	42.5	0.32										
<b><math>Z = 82</math> (Pb)</b>																											
155	237	0.225	0.02	7.5	0.01	155	242	0.225	0.02	12.5	0.10	117	207	0.200	0.04	50.0	0.08										
156	238	0.200	0.02	12.5	0.03	156	243	0.225	0.02	17.5	0.17	123	213	0.075	0.02	55.0	0.01										
157	239	0.200	0.02	15.0	0.07	157	244	0.225	0.02	17.5	0.20	155	245	0.225	0.00	10.0	0.06										
158	240	0.175	0.02	15.0	0.11	158	245	0.200	0.02	17.5	0.21	156	246	0.225	0.02	12.5	0.14										
159	241	0.175	0.04	12.5	0.03	159	246	0.200	0.02	17.5	0.14	157	247	0.225	0.02	15.0	0.26										
<b><math>Z = 83</math> (Bi)</b>																											
111	194	0.075	0.00	17.5	0.02	<b><math>Z = 88</math> (Ra)</b>																					
112	195	0.050	0.00	30.0	0.02	109	197	0.250	0.04	20.0	0.11	160	250	0.225	0.04	20.0	0.02										
113	196	0.050	0.00	27.5	0.03	110	198	0.250	0.00	47.5	0.09	<b><math>Z = 91</math> (Pa)</b>															
114	197	0.050	0.00	30.0	0.01	111	199	0.225	0.00	45.0	0.09	109	200	0.275	0.02	15.0	0.23										
156	239	0.200	0.02	15.0	0.13	112	200	0.225	0.00	47.5	0.07	110	201	0.300	0.02	12.5	0.16										
157	240	0.200	0.02	15.0	0.09	113	201	0.225	0.02	45.0	0.11	111	202	0.325	0.02	15.0	0.24										
158	241	0.175	0.02	17.5	0.11	114	202	0.225	0.02	47.5	0.09	112	203	0.225	0.02	30.0	0.23										
159	242	0.175	0.02	17.5	0.06	115	203	0.200	0.02	45.0	0.13	113	204	0.225	0.02	35.0	0.38										
160	243	0.175	0.04	12.5	0.02	117	205	0.200	0.02	52.5	0.03	114	205	0.225	0.02	37.5	0.40										
<b><math>Z = 84</math> (Po)</b>																											
97	181	0.225	-0.04	17.5	0.15	154	242	0.225	0.00	10.0	0.02	115	206	0.225	0.04	40.0	0.32										
98	182	0.275	-0.02	12.5	0.06	156	244	0.225	0.02	15.0	0.17	117	208	0.200	0.04	47.5	0.16										
155	239	0.225	0.02	10.0	0.05	157	245	0.225	0.02	17.5	0.23	123	214	0.075	0.02	52.5	0.01										
156	240	0.200	0.02	12.5	0.07	158	246	0.225	0.02	20.0	0.18	155	246	0.225	0.00	10.0	0.04										
157	241	0.200	0.02	15.0	0.13	159	247	0.200	0.02	17.5	0.14	156	247	0.225	0.00	12.5	0.12										
158	242	0.200	0.02	20.0	0.06	160	248	0.200	0.04	12.5	0.04	157	248	0.225	0.02	15.0	0.23										

Table 1: Continued. Calculated Effect of Triaxiality on Ground-State Masses and Deformations

$N$	$A$	$\epsilon_2$	$\epsilon_4$	$\gamma$	$\Delta E_\gamma$ (MeV)	$N$	$A$	$\epsilon_2$	$\epsilon_4$	$\gamma$	$\Delta E_\gamma$ (MeV)	$N$	$A$	$\epsilon_2$	$\epsilon_4$	$\gamma$	$\Delta E_\gamma$ (MeV)
<b><math>Z = 91</math> (Pa)</b>						<b><math>Z = 97</math> (Bk)</b>						<b><math>Z = 103</math> (Lr)</b>					
158	249	0.225	0.02	17.5	0.22	123	220	0.100	0.02	50.0	0.02	139	242	0.250	0.00	15.0	0.25
159	250	0.225	0.02	17.5	0.11	129	226	0.350	0.02	25.0	0.53	140	243	0.250	0.00	15.0	0.15
160	251	0.225	0.04	17.5	0.07	130	227	0.350	0.02	25.0	0.35	141	244	0.250	0.00	15.0	0.07
<b><math>Z = 92</math> (U)</b>						131	228	0.350	0.02	25.0	0.37	<b><math>Z = 104</math> (Rf)</b>					
111	203	0.300	0.02	15.0	0.25	132	229	0.325	0.02	22.5	0.26	138	242	0.250	0.00	15.0	0.18
112	204	0.325	0.02	17.5	0.11	133	230	0.325	0.02	20.0	0.18	139	243	0.250	0.00	15.0	0.26
113	205	0.225	0.02	30.0	0.22	<b><math>Z = 98</math> (Cf)</b>						140	244	0.250	0.00	15.0	0.16
114	206	0.225	0.04	37.5	0.36	123	221	0.100	0.02	50.0	0.02	141	245	0.250	0.00	15.0	0.10
115	207	0.225	0.04	37.5	0.24	129	227	0.325	0.02	25.0	0.31	<b><math>Z = 105</math> (Db)</b>					
116	208	0.225	0.04	40.0	0.19	130	228	0.350	0.02	25.0	0.29	138	243	0.250	0.00	15.0	0.03
117	209	0.225	0.06	47.5	0.05	131	229	0.350	0.02	25.0	0.35	139	244	0.250	0.00	15.0	0.14
123	215	0.075	0.02	52.5	0.02	132	230	0.325	0.02	22.5	0.37	140	245	0.225	0.00	10.0	0.07
156	248	0.225	0.00	10.0	0.06	133	231	0.325	0.02	20.0	0.38	141	246	0.225	0.00	5.0	0.01
157	249	0.225	0.02	12.5	0.16	134	232	0.325	0.02	20.0	0.27	<b><math>Z = 106</math> (Sg)</b>					
158	250	0.225	0.02	15.0	0.24	135	233	0.300	0.02	17.5	0.10	139	245	0.250	0.02	12.5	0.07
159	251	0.225	0.02	17.5	0.05	136	234	0.300	0.02	20.0	0.06	140	246	0.250	0.02	12.5	0.13
<b><math>Z = 93</math> (Np)</b>						138	236	0.300	0.02	22.5	0.01	141	247	0.250	0.02	12.5	0.09
113	206	0.250	0.04	35.0	0.08	141	239	0.225	-0.04	5.0	0.02	<b><math>Z = 107</math> (Ns)</b>					
114	207	0.250	0.04	37.5	0.15	<b><math>Z = 99</math> (Es)</b>						140	247	0.250	0.02	12.5	0.11
115	208	0.225	0.04	37.5	0.24	132	231	0.325	0.02	25.0	0.05	141	248	0.250	0.02	12.5	0.17
116	209	0.225	0.04	40.0	0.14	133	232	0.325	0.02	27.5	0.02	142	249	0.250	0.02	12.5	0.02
117	210	0.150	0.00	7.5	0.02	134	233	0.325	0.02	25.0	0.02	<b><math>Z = 108</math> (Hs)</b>					
119	212	0.175	0.02	55.0	0.02	136	235	0.300	0.02	25.0	0.04	142	250	0.225	0.02	7.5	0.03
156	249	0.225	0.00	7.5	0.03	137	236	0.225	-0.04	10.0	0.11						
157	250	0.225	0.02	12.5	0.13	138	237	0.225	-0.04	10.0	0.09						
158	251	0.225	0.02	15.0	0.24	139	238	0.225	-0.04	10.0	0.07						
159	252	0.225	0.02	15.0	0.08	140	239	0.225	-0.04	7.5	0.04						
160	253	0.225	0.04	15.0	0.02	141	240	0.225	-0.04	5.0	0.03						
<b><math>Z = 94</math> (Pu)</b>						<b><math>Z = 100</math> (Fm)</b>											
115	209	0.175	0.00	15.0	0.08	136	236	0.250	-0.02	12.5	0.08						
116	210	0.225	0.04	37.5	0.03	137	237	0.250	-0.02	15.0	0.16						
117	211	0.150	0.02	5.0	0.02	138	238	0.250	-0.02	12.5	0.21						
157	251	0.225	0.02	10.0	0.05	139	239	0.250	-0.02	12.5	0.24						
158	252	0.225	0.02	12.5	0.10	140	240	0.250	-0.02	12.5	0.06						
<b><math>Z = 95</math> (Am)</b>						141	241	0.225	-0.02	5.0	0.01						
117	212	0.150	0.02	5.0	0.02	<b><math>Z = 101</math> (Md)</b>											
121	216	0.125	0.02	52.5	0.01	136	237	0.250	-0.02	15.0	0.05						
123	218	0.100	0.02	52.5	0.02	137	238	0.250	-0.02	15.0	0.16						
131	226	0.350	0.02	25.0	0.08	138	239	0.250	-0.02	15.0	0.18						
156	251	0.225	0.02	5.0	0.02	139	240	0.250	-0.02	15.0	0.25						
157	252	0.225	0.02	7.5	0.05	140	241	0.225	-0.02	10.0	0.07						
158	253	0.225	0.02	10.0	0.08	141	242	0.225	-0.02	7.5	0.03						
<b><math>Z = 96</math> (Cm)</b>						<b><math>Z = 102</math> (No)</b>											
123	219	0.100	0.02	52.5	0.02	137	239	0.250	0.00	15.0	0.04						
130	226	0.350	0.02	25.0	0.40	138	240	0.250	0.00	15.0	0.18						
131	227	0.350	0.02	25.0	0.31	139	241	0.250	-0.02	15.0	0.23						
<b><math>Z = 97</math> (Bk)</b>						140	242	0.225	-0.02	10.0	0.09						
121	218	0.125	0.02	47.5	0.05	141	243	0.225	-0.02	7.5	0.03						
122	219	0.125	0.02	47.5	0.04	<b><math>Z = 103</math> (Lr)</b>					138	241	0.250	0.00	15.0	0.17	

## EXPLANATION OF TABLE 2

**Table 2 Calculated Effect of Reflection Asymmetry on Nuclear Ground-State Masses and Deformations**

$Z$	Proton number. The table is ordered by increasing proton number. The corresponding chemical symbol of each named element is given in parentheses.
$N$	Neutron number.
$A$	Mass Number.
$\epsilon_2$	Calculated ground-state quadrupole deformation in the Nilsson perturbed-spheroid parameterization.
$\epsilon_3$	Calculated ground-state octupole deformation in the Nilsson perturbed-spheroid parameterization.
$\epsilon_4$	Calculated ground-state hexadecapole deformation in the Nilsson perturbed-spheroid parameterization.
$\epsilon_6$	Calculated ground-state hexacontatetrapole deformation in the Nilsson perturbed-spheroid parameterization.
$\Delta E_{\epsilon_3}$	Calculated decrease in potential energy due to reflection asymmetry.  We only present nuclei for which the calculated decrease in energy due to reflection asymmetry is equal to or larger than 0.01 MeV. In contrast to the calculation leading to our FRDM(1992) mass table [1] the ground-state determination here is based on calculations in a full 4D space. The accuracy of the calculation is 0.005 in each of the 4 deformation parameters.

Table 2: Calculated Effect of Reflection Asymmetry on Nuclear Ground-State Masses and Deformations

$N$	$A$	$\epsilon_2$	$\epsilon_3$	$\epsilon_4$	$\epsilon_6$	$\Delta E_{\epsilon_3}$ (MeV)	$N$	$A$	$\epsilon_2$	$\epsilon_3$	$\epsilon_4$	$\epsilon_6$	$\Delta E_{\epsilon_3}$ (MeV)	$N$	$A$	$\epsilon_2$	$\epsilon_3$	$\epsilon_4$	$\epsilon_6$	$\Delta E_{\epsilon_3}$ (MeV)														
<b><math>Z = 8</math> (O )</b>																																		
8	16	-0.03	0.20	0.12	-0.02	0.08	89	133	0.11	0.03	-0.03	0.00	0.13	88	144	0.15	0.09	-0.05	0.02	0.49														
<b><math>Z = 15</math> (P )</b>																																		
8	23	-0.02	0.02	0.12	-0.03	0.01	89	134	0.11	0.02	-0.03	0.00	0.19	90	146	0.16	0.09	-0.05	0.02	0.57														
<b><math>Z = 17</math> (Cl)</b>																																		
8	25	-0.05	0.13	0.02	0.00	0.03	42	90	-0.01	0.04	0.00	0.00	0.04	131	187	0.10	0.06	-0.05	0.00	0.11														
<b><math>Z = 19</math> (K )</b>																																		
16	35	-0.03	0.02	0.00	-0.04	0.01	55	108	0.14	0.05	-0.05	0.02	0.04	133	189	0.11	0.09	-0.06	0.01	0.64														
41	60	-0.07	0.07	0.00	0.00	0.03	56	109	0.15	0.06	-0.04	0.02	0.06	<b><math>Z = 57</math> (La)</b>																				
43	62	-0.08	0.05	0.02	0.00	0.02	57	110	0.16	0.06	-0.03	0.02	0.12	53	110	0.17	0.06	-0.05	0.02	0.14														
<b><math>Z = 20</math> (Ca)</b>																																		
36	56	-0.07	0.02	0.02	0.02	0.04	59	112	0.17	0.04	-0.03	0.02	0.05	55	112	0.18	0.10	-0.04	0.04	0.35														
37	57	-0.07	0.03	0.01	0.00	0.02	90	143	0.14	0.06	-0.05	0.01	0.02	56	113	0.20	0.10	-0.03	0.04	0.38														
39	59	0.00	0.05	0.00	0.00	0.01	91	144	0.14	0.07	-0.05	0.01	0.01	57	114	0.21	0.08	-0.05	0.04	0.24														
40	60	0.00	0.07	0.00	0.00	0.03	<b><math>Z = 54</math> (Xe)</b>																											
41	61	-0.02	0.09	0.00	0.00	0.05	54	108	0.15	0.05	-0.05	0.02	0.05	85	142	0.10	0.06	-0.03	0.00	0.15														
<b><math>Z = 21</math> (Sc)</b>																																		
38	59	-0.07	0.03	0.01	0.01	0.01	56	110	0.16	0.07	-0.04	0.03	0.20	87	144	0.14	0.09	-0.05	0.01	0.41														
39	60	-0.04	0.06	0.00	0.00	0.02	57	111	0.17	0.08	-0.03	0.03	0.23	88	145	0.16	0.09	-0.05	0.02	0.53														
40	61	-0.02	0.08	0.00	0.00	0.03	58	112	0.18	0.07	-0.03	0.03	0.14	89	146	0.16	0.10	-0.04	0.02	0.48														
41	62	-0.04	0.09	-0.01	0.00	0.06	59	113	0.19	0.06	-0.03	0.03	0.10	90	147	0.17	0.09	-0.05	0.02	0.32														
<b><math>Z = 36</math> (Kr)</b>																																		
87	123	0.08	0.05	0.00	0.00	0.02	88	142	0.13	0.06	-0.06	0.01	0.11	131	188	0.10	0.07	-0.04	0.00	0.28														
88	124	0.10	0.07	0.00	0.00	0.12	89	143	0.14	0.08	-0.05	0.01	0.18	132	189	0.11	0.08	-0.05	0.00	0.48														
<b><math>Z = 37</math> (Rb)</b>																																		
87	124	0.08	0.07	0.00	0.00	0.05	91	145	0.16	0.08	-0.05	0.02	0.11	134	191	0.13	0.10	-0.05	0.01	0.76														
88	125	0.09	0.08	0.00	0.00	0.19	<b><math>Z = 55</math> (Cs)</b>																											
89	126	0.11	0.09	-0.01	0.00	0.54	52	107	0.12	0.04	-0.05	0.01	0.01	<b><math>Z = 58</math> (Ce)</b>																				
90	127	0.11	0.09	-0.02	0.00	0.43	53	108	0.15	0.07	-0.05	0.02	0.13	55	113	0.20	0.08	-0.04	0.04	0.31														
<b><math>Z = 38</math> (Sr)</b>																																		
87	125	0.05	0.07	0.00	0.00	0.03	55	110	0.16	0.09	-0.04	0.03	0.39	85	143	0.12	0.06	-0.03	0.00	0.14														
88	126	0.07	0.09	-0.01	0.00	0.17	56	111	0.17	0.09	-0.04	0.03	0.41	86	144	0.13	0.07	-0.04	0.01	0.22														
89	127	0.10	0.10	-0.02	0.00	0.41	57	112	0.18	0.09	-0.03	0.03	0.41	87	145	0.15	0.08	-0.04	0.01	0.38														
90	128	0.10	0.10	-0.02	0.01	0.59	58	113	0.19	0.09	-0.03	0.03	0.30	88	146	0.16	0.09	-0.05	0.02	0.46														
<b><math>Z = 39</math> (Y )</b>																																		
87	126	0.03	0.07	-0.01	0.00	0.04	85	140	0.09	0.03	-0.04	-0.01	0.01	90	148	0.19	0.07	-0.05	0.02	0.02														
88	127	0.04	0.09	-0.01	0.01	0.20	86	141	0.11	0.04	-0.05	0.00	0.06	131	189	0.10	0.08	-0.04	0.00	0.40														
89	128	0.04	0.11	-0.01	0.01	0.51	87	142	0.13	0.07	-0.05	0.01	0.20	132	190	0.11	0.08	-0.04	0.00	0.57														
90	129	0.04	0.12	-0.01	0.02	0.61	88	143	0.14	0.08	-0.06	0.01	0.35	133	191	0.12	0.09	-0.05	0.01	0.85														
91	130	0.09	0.13	-0.03	0.01	0.24	89	144	0.15	0.09	-0.05	0.02	0.49	134	192	0.13	0.10	-0.05	0.01	0.83														
<b><math>Z = 40</math> (Zr)</b>																																		
88	128	0.03	0.09	-0.01	0.01	0.13	91	146	0.16	0.09	-0.05	0.02	0.24	136	194	0.15	0.10	-0.05	0.02	0.14														
89	129	0.03	0.11	-0.01	0.01	0.45	92	147	0.19	0.04	-0.07	0.01	0.02	<b><math>Z = 59</math> (Pr)</b>																				
90	130	0.03	0.12	-0.01	0.02	0.54	<b><math>Z = 56</math> (Ba)</b>																											
91	131	0.04	0.13	-0.02	0.01	0.16	52	108	0.13	0.05	-0.05	0.01	0.05	86	145	0.12	0.07	-0.03	0.00	0.21														
<b><math>Z = 41</math> (Nb)</b>																																		
87	128	0.03	0.05	-0.01	0.00	0.07	54	110	0.17	0.09	-0.04	0.03	0.34	88	147	0.17	0.07	-0.05	0.02	0.26														
88	129	0.03	0.07	-0.01	0.00	0.13	55	111	0.17	0.10	-0.04	0.03	0.47	89	148	0.19	0.05	-0.06	0.02	0.06														
89	130	0.01	0.11	-0.01	0.02	0.26	56	112	0.18	0.10	-0.03	0.04	0.48	130	189	0.07	0.07	-0.03	0.00	0.12														
90	131	0.00	0.12	-0.02	0.02	0.02	57	113	0.19	0.10	-0.03	0.04	0.44	131	190	0.09	0.09	-0.03	0.00	0.58														
<b><math>Z = 42</math> (Mo)</b>																																		
89	131	0.02	0.09	-0.01	0.02	0.22	85	141	0.09	0.05	-0.04	0.00	0.04	133	192	0.11	0.10	-0.05	0.01	0.92														
90	132	0.00	0.10	-0.01	0.01	0.11	86	142	0.12	0.06	-0.05	0.01																						

Table 2: Continued. Calculated Effect of Reflection Asymmetry on Nuclear Ground-State Masses and Deformations

$N$	$A$	$\epsilon_2$	$\epsilon_3$	$\epsilon_4$	$\epsilon_6$	$\Delta E_{\epsilon_3}$ (MeV)	$N$	$A$	$\epsilon_2$	$\epsilon_3$	$\epsilon_4$	$\epsilon_6$	$\Delta E_{\epsilon_3}$ (MeV)	$N$	$A$	$\epsilon_2$	$\epsilon_3$	$\epsilon_4$	$\epsilon_6$	$\Delta E_{\epsilon_3}$ (MeV)							
<b><math>Z = 60</math> (Nd)</b>																											
85	145	0.10	0.07	-0.02	0.00	0.10	133	198	0.11	0.08	-0.04	0.00	0.47	136	216	0.06	0.05	-0.01	0.00	0.02							
86	146	0.14	0.06	-0.04	0.00	0.08	134	199	0.13	0.08	-0.05	0.01	0.17	137	217	0.07	0.06	-0.02	0.00	0.17							
87	147	0.16	0.06	-0.04	0.01	0.08	<b><math>Z = 66</math> (Dy)</b>																				
88	148	0.18	0.06	-0.05	0.02	0.09	129	195	0.03	0.06	-0.01	0.00	0.15	138	218	0.08	0.05	-0.02	0.00	0.14							
130	190	0.07	0.07	-0.03	0.00	0.14	130	196	0.05	0.08	-0.02	0.00	0.35	139	219	0.09	0.05	-0.02	0.00	0.09							
131	191	0.09	0.09	-0.03	0.00	0.67	131	197	0.07	0.09	-0.02	0.01	0.41	94	175	0.07	0.02	0.00	0.00	0.02							
132	192	0.10	0.09	-0.03	0.00	0.75	132	198	0.08	0.10	-0.02	0.01	0.29	135	216	0.02	0.05	-0.01	0.00	0.05							
133	193	0.11	0.09	-0.05	0.00	0.86	133	199	0.11	0.08	-0.04	0.00	0.36	136	217	0.03	0.06	0.00	0.00	0.06							
134	194	0.13	0.10	-0.05	0.01	0.64	134	200	0.11	0.08	-0.04	0.00	0.13	137	218	0.05	0.06	-0.01	0.00	0.18							
135	195	0.14	0.10	-0.05	0.02	0.18	<b><math>Z = 67</math> (Ho)</b>																				
<b><math>Z = 61</math> (Pm)</b>																											
85	146	0.09	0.07	-0.02	0.00	0.03	130	197	0.07	0.06	-0.02	0.00	0.17	139	220	0.07	0.06	-0.01	0.01	0.24							
86	147	0.16	0.03	-0.04	0.00	0.02	131	198	0.07	0.09	-0.02	0.01	0.13	140	221	0.07	0.05	-0.01	0.00	0.13							
87	148	0.17	0.05	-0.04	0.01	0.06	132	199	0.11	0.05	-0.04	-0.01	0.10	97	179	0.01	0.04	0.00	0.00	0.04							
88	149	0.19	0.04	-0.05	0.02	0.09	133	200	0.11	0.07	-0.04	0.00	0.20	98	180	0.00	0.03	0.00	0.00	0.02							
129	190	0.04	0.05	-0.01	0.00	0.03	134	201	0.13	0.05	-0.05	0.00	0.04	99	181	0.02	0.03	0.00	0.00	0.10							
130	191	0.07	0.08	-0.03	0.00	0.34	<b><math>Z = 68</math> (Er)</b>																				
131	192	0.08	0.09	-0.03	0.00	0.82	129	197	0.03	0.04	-0.01	0.00	0.03	101	183	-0.01	0.04	-0.01	0.00	0.06							
132	193	0.10	0.09	-0.03	0.00	0.83	130	198	0.06	0.05	-0.02	0.00	0.10	102	184	0.00	0.02	-0.01	0.00	0.04							
133	194	0.11	0.10	-0.04	0.01	0.87	131	199	0.07	0.08	-0.02	0.00	0.08	134	216	0.01	0.04	0.00	0.00	0.02							
134	195	0.12	0.10	-0.05	0.01	0.55	132	200	0.11	0.04	-0.04	-0.01	0.05	135	217	0.02	0.07	-0.01	0.01	0.16							
135	196	0.13	0.10	-0.05	0.01	0.05	133	201	0.11	0.06	-0.04	0.00	0.16	136	218	0.01	0.06	0.00	0.00	0.16							
<b><math>Z = 62</math> (Sm)</b>																											
87	149	0.17	0.03	-0.04	0.01	0.02	130	199	0.06	0.05	-0.02	0.00	0.01	138	220	0.01	0.07	-0.01	0.00	0.23							
88	150	0.19	0.04	-0.04	0.02	0.02	130	199	0.06	0.05	-0.02	0.00	0.01	139	221	0.03	0.07	-0.01	0.01	0.34							
89	151	0.21	0.02	-0.05	0.02	0.01	133	202	0.11	0.05	-0.04	0.00	0.06	140	222	0.01	0.07	0.00	0.01	0.26							
129	191	0.04	0.06	-0.01	0.00	0.09	<b><math>Z = 70</math> (Yb)</b>																				
130	192	0.07	0.08	-0.02	0.00	0.40	133	203	0.11	0.05	-0.04	0.00	0.04	95	178	0.07	0.07	-0.01	0.00	0.20							
131	193	0.08	0.09	-0.03	0.00	0.81	134	204	0.11	0.04	-0.04	0.00	0.04	96	179	0.07	0.07	-0.01	0.00	0.09							
132	194	0.09	0.10	-0.03	0.01	0.78	<b><math>Z = 72</math> (Hf)</b>																				
133	195	0.10	0.09	-0.04	0.00	0.79	133	205	0.11	0.04	-0.03	-0.01	0.01	133	216	0.04	0.09	-0.02	0.00	0.12							
134	196	0.12	0.10	-0.04	0.01	0.45	<b><math>Z = 73</math> (Ta)</b>																				
135	208	0.11	0.03	-0.03	0.00	0.08	135	208	0.11	0.03	-0.03	0.00	0.08	135	218	0.05	0.08	-0.02	0.00	0.32							
<b><math>Z = 63</math> (Eu)</b>																											
84	147	0.04	0.05	-0.01	0.00	0.02	135	209	0.11	0.04	-0.03	0.00	0.04	136	219	0.05	0.08	-0.02	0.00	0.25							
129	192	0.04	0.07	-0.02	0.00	0.23	135	210	0.11	0.03	-0.03	0.00	0.04	137	220	0.07	0.08	-0.03	0.00	0.38							
130	193	0.06	0.09	-0.02	0.00	0.54	<b><math>Z = 75</math> (Re)</b>																				
131	194	0.07	0.10	-0.03	0.01	0.85	135	210	0.11	0.03	-0.03	0.00	0.03	138	221	0.08	0.08	-0.03	0.00	0.28							
132	195	0.08	0.10	-0.03	0.01	0.79	<b><math>Z = 76</math> (Os)</b>																				
133	196	0.10	0.10	-0.04	0.01	0.71	134	210	0.09	0.02	-0.02	-0.01	0.02	133	217	0.04	0.09	-0.02	0.00	0.34							
134	197	0.11	0.10	-0.05	0.01	0.36	135	211	0.11	0.04	-0.02	0.00	0.05	134	218	0.05	0.09	-0.02	0.00	0.44							
<b><math>Z = 64</math> (Gd)</b>																											
129	193	0.04	0.07	-0.02	0.00	0.22	135	212	0.10	0.03	-0.02	-0.01	0.04	135	219	0.08	0.08	-0.04	0.00	0.46							
130	194	0.05	0.08	-0.02	0.00	0.51	136	213	0.11	0.03	-0.02	0.00	0.02	137	221	0.09	0.09	-0.04	0.00	0.32							
131	195	0.07	0.10	-0.02	0.01	0.72	<b><math>Z = 78</math> (Pt)</b>																				
132	196	0.08	0.10	-0.03	0.01	0.64	135	213	0.09	0.04	-0.02	0.00	0.08	135	219	0.08	0.08	-0.04	0.00	0.46							
133	197	0.10	0.09	-0.04	0.00	0.62	136	214	0.09	0.03	-0.02	0.00	0.03	131	216	0.05	0.09	-0.03	0.00	0.29							
134	198	0.12	0.09	-0.05	0.01	0.29	137	215	0.11	0.03	-0.03	0.00	0.02	132	217	0.06	0.10	-0.03	0.00	0.53							
<b><math>Z = 65</math> (Tb)</b>																											
128	193	0.01	0.02	0.00	0.00	0.06	135	214	0.07	0.04	-0.02	0.00	0.07	134	219	0.09	0.09	-0.05	-0.01	0.64							
129	194	0.03	0.05	-0.01	0.01	0.22	136	215	0.08	0.04	-0.02	0.00	0.08	135	220	0.10	0.09	-0.0									

Table 2: Continued. Calculated Effect of Reflection Asymmetry on Nuclear Ground-State Masses and Deformations

$N$	$A$	$\epsilon_2$	$\epsilon_3$	$\epsilon_4$	$\epsilon_6$	$\Delta E_{\epsilon_3}$ (MeV)	$N$	$A$	$\epsilon_2$	$\epsilon_3$	$\epsilon_4$	$\epsilon_6$	$\Delta E_{\epsilon_3}$ (MeV)	$N$	$A$	$\epsilon_2$	$\epsilon_3$	$\epsilon_4$	$\epsilon_6$	$\Delta E_{\epsilon_3}$ (MeV)														
<b><math>Z = 85</math> (At)</b>																																		
139	224	0.13	0.04	-0.07	-0.01	0.07	138	227	0.15	0.08	-0.07	0.01	0.33	126	221	0.01	0.04	0.00	0.00	0.11														
140	225	0.14	0.02	-0.07	-0.01	0.03	139	228	0.16	0.07	-0.07	0.01	0.13	127	222	0.04	0.07	-0.01	0.00	0.44														
141	226	0.15	0.02	-0.07	0.00	0.03	<b><math>Z = 90</math> (Th)</b>																											
<b><math>Z = 86</math> (Rn)</b>																																		
131	217	0.06	0.10	-0.03	0.00	0.59	129	219	0.07	0.09	-0.03	0.00	0.72	129	224	0.07	0.10	-0.02	0.01	1.14														
132	218	0.07	0.10	-0.04	0.00	0.67	130	220	0.08	0.10	-0.04	0.00	1.33	130	225	0.09	0.10	-0.03	0.01	0.95														
133	219	0.09	0.09	-0.05	-0.01	0.85	131	221	0.10	0.09	-0.05	0.00	1.31	131	226	0.10	0.11	-0.03	0.01	0.57														
134	220	0.10	0.09	-0.05	0.00	0.85	132	222	0.10	0.10	-0.05	0.00	1.35	132	227	0.12	0.10	-0.04	0.01	0.21														
135	221	0.10	0.09	-0.05	0.00	0.82	133	223	0.12	0.10	-0.06	0.00	1.42	133	228	0.14	0.09	-0.05	0.01	0.11														
136	222	0.10	0.09	-0.05	0.00	0.64	134	224	0.13	0.11	-0.06	0.01	1.22	<b><math>Z = 96</math> (Cm)</b>																				
137	223	0.13	0.09	-0.06	0.00	0.47	135	225	0.13	0.10	-0.06	0.01	0.91	125	221	0.02	0.03	0.00	0.00	0.01														
138	224	0.13	0.08	-0.06	0.00	0.29	136	226	0.14	0.10	-0.06	0.01	0.50	126	222	0.00	0.03	0.00	0.00	0.02														
139	225	0.15	0.05	-0.07	0.00	0.12	137	227	0.15	0.10	-0.06	0.02	0.27	127	223	0.03	0.07	-0.01	0.00	0.37														
140	226	0.15	0.04	-0.07	0.00	0.09	138	228	0.16	0.08	-0.07	0.01	0.08	128	224	0.04	0.08	-0.01	0.00	0.52														
141	227	0.16	0.02	-0.07	0.00	0.03	<b><math>Z = 91</math> (Pa)</b>																											
146	232	0.21	0.02	-0.05	0.03	0.02	129	220	0.08	0.09	-0.04	0.00	1.14	130	226	0.08	0.10	-0.03	0.01	0.84														
<b><math>Z = 87</math> (Fr)</b>																																		
130	217	0.07	0.09	-0.04	-0.01	0.34	132	223	0.11	0.10	-0.05	0.00	1.36	<b><math>Z = 97</math> (Bk)</b>																				
131	218	0.08	0.10	-0.04	0.00	1.20	133	224	0.12	0.10	-0.06	0.01	1.35	125	222	0.03	0.04	0.00	0.00	0.07														
132	219	0.09	0.10	-0.05	0.00	1.04	134	225	0.13	0.11	-0.06	0.01	0.99	126	223	0.01	0.05	0.00	0.00	0.14														
133	220	0.10	0.09	-0.06	-0.01	1.20	135	226	0.14	0.11	-0.06	0.02	0.61	127	224	0.03	0.07	-0.01	0.00	0.55														
134	221	0.10	0.10	-0.06	0.00	1.14	136	227	0.14	0.10	-0.06	0.02	0.27	128	225	0.04	0.08	-0.01	0.00	0.75														
135	222	0.11	0.10	-0.06	0.00	1.05	137	228	0.15	0.10	-0.06	0.02	0.04	129	226	0.06	0.10	-0.02	0.01	0.87														
136	223	0.12	0.10	-0.06	0.01	0.90	<b><math>Z = 92</math> (U)</b>																											
137	224	0.13	0.10	-0.06	0.01	0.67	127	219	0.02	0.04	-0.01	0.00	0.04	131	228	0.09	0.11	-0.03	0.01	0.01														
138	225	0.14	0.09	-0.06	0.01	0.41	128	220	0.05	0.08	-0.02	0.00	0.08	<b><math>Z = 98</math> (Cf)</b>																				
139	226	0.15	0.06	-0.07	0.00	0.22	129	221	0.08	0.09	-0.03	0.00	1.16	125	223	0.03	0.04	0.00	0.00	0.04														
140	227	0.15	0.05	-0.07	0.00	0.13	130	222	0.09	0.10	-0.04	0.01	1.21	126	224	0.00	0.05	0.00	0.00	0.10														
141	228	0.16	0.03	-0.07	0.00	0.06	131	223	0.10	0.10	-0.04	0.01	1.27	127	225	0.03	0.07	-0.01	0.00	0.47														
<b><math>Z = 88</math> (Ra)</b>																																		
129	217	0.05	0.08	-0.03	0.00	0.13	132	224	0.12	0.10	-0.05	0.01	1.22	128	226	0.03	0.08	-0.01	0.01	0.56														
130	218	0.07	0.09	-0.04	0.00	0.59	133	225	0.13	0.10	-0.06	0.01	1.06	129	227	0.05	0.09	-0.01	0.01	0.68														
131	219	0.08	0.10	-0.04	0.00	1.06	134	226	0.13	0.10	-0.06	0.01	0.60	130	228	0.07	0.10	-0.02	0.01	0.06														
132	220	0.10	0.09	-0.06	-0.01	1.20	135	227	0.14	0.10	-0.06	0.02	0.30	<b><math>Z = 99</math> (Es)</b>																				
133	221	0.10	0.10	-0.06	0.00	1.35	127	220	0.03	0.06	-0.01	0.00	0.22	126	225	0.00	0.06	0.00	0.00	0.20														
134	222	0.11	0.10	-0.06	0.00	1.27	128	221	0.05	0.08	-0.02	0.00	0.48	127	226	0.02	0.07	-0.01	0.00	0.61														
135	223	0.12	0.10	-0.06	0.01	1.17	129	222	0.08	0.09	-0.03	0.00	1.21	128	227	0.03	0.08	-0.01	0.01	0.71														
136	224	0.13	0.10	-0.06	0.01	0.91	130	223	0.09	0.10	-0.03	0.01	1.19	129	228	0.04	0.09	-0.01	0.01	0.21														
137	225	0.14	0.10	-0.06	0.01	0.63	131	224	0.10	0.11	-0.03	0.01	1.23	<b><math>Z = 100</math> (Fm)</b>																				
138	226	0.15	0.08	-0.07	0.01	0.40	132	225	0.12	0.10	-0.05	0.01	0.87	126	226	0.00	0.06	0.00	0.00	0.12														
139	227	0.16	0.07	-0.07	0.01	0.20	133	226	0.13	0.09	-0.06	0.01	0.63	127	227	0.01	0.07	-0.01	0.00	0.47														
140	228	0.16	0.06	-0.07	0.01	0.08	134	227	0.14	0.10	-0.06	0.02	0.23	128	228	0.02	0.08	-0.01	0.01	0.52														
141	229	0.17	0.02	-0.08	0.01	0.03	135	228	0.15	0.10	-0.06	0.02	0.01	129	229	0.04	0.09	-0.01	0.01	0.28														
<b><math>Z = 89</math> (Ac)</b>																																		
129	218	0.07	0.09	-0.04	0.00	0.58	127	221	0.03	0.06	-0.01	0.00	0.21	128	229	0.01	0.08	-0.01	0.00	0.61														
130	219	0.08	0.10	-0.04	0.00	1.18	128	222	0.05	0.08	-0.02	0.00	0.35	129	230	0.02	0.09	-0.01	0.01	0.23														
131	220	0.09	0.10	-0.05	0.00	1.28	129	223	0.07	0.09	-0.02	0.00	1.14	<b><math>Z = 94</math> (Pu)</b>																				
132	221	0.10	0.10	-0.05	0.00	1.42	130	224	0.09	0.10	-0.03	0.01	1.09	131	225	0.10	0.11	-0.03	0.01	0.94														
133	222	0.11	0.10	-0.06	0.00	1.43	131	225	0.10	0.11	-0.03	0.01	0.94	132	226																			

## EXPLANATION OF GRAPHS

Graph 1 Four calculated potential-energy surfaces versus  $\varepsilon_2$  and  $\gamma$  (minimized with respect to  $\varepsilon_4$ ).

Minima are indicated by colored round dots, saddle points by pairs of crossed lines. The numbers on a blue background give the energy in MeV of the thicker contour lines which are spaced 1 MeV apart; the spacing between the thinner lines is 0.2 MeV. For the Th diagram the intervals are doubled. To obtain a suitable range of values in the plotted surfaces we have, following standard practice, subtracted the energy obtained for a spherical shape in the macroscopic part of the model. This normalization has the additional advantage that the ground-state mass can be obtained as the sum of the energy of the minimum in the plot and the macroscopic energy of the nucleus for a spherical shape. The surfaces exhibit typical structures that we obtain in our current investigation. Each point in a surface corresponds to the energy of a specific nuclear shape. The lower left tip of the pie-like plot corresponds to a spherical shape. Points along the upper straight line correspond to oblate shapes (like a discus) and those along the lower straight line to prolate shapes (like an American football). The energy values in the interior of the pie are calculated for axially-asymmetric nuclear shapes (a somewhat simplified analogy is that these points correspond to shapes that result from standing on a football). Shapes corresponding to the three minima and one of the saddle points of  $^{216}\text{Th}$  are shown at the top in the colors of the symbols at their respective locations in the contour plot. Shapes at equivalent locations in the other plots are similar, but not exactly identical, due to possible differences in the  $\varepsilon_4$  shape coordinate. In subplot (3)  $^{216}\text{Th}$  exhibits triple shape coexistence. The lowest minimum is spherical (blue dot), the next higher one oblate (green dot), and finally there is a triaxial minimum, close to the prolate axis (red dot). Our immersion-analysis program has identified as optimum saddle points between pairs of minima the locations indicated by the crossed-lines symbols.

Graph 2 Calculated ground-state axial asymmetry instability for nuclei in the range  $47 < N < 143$ .

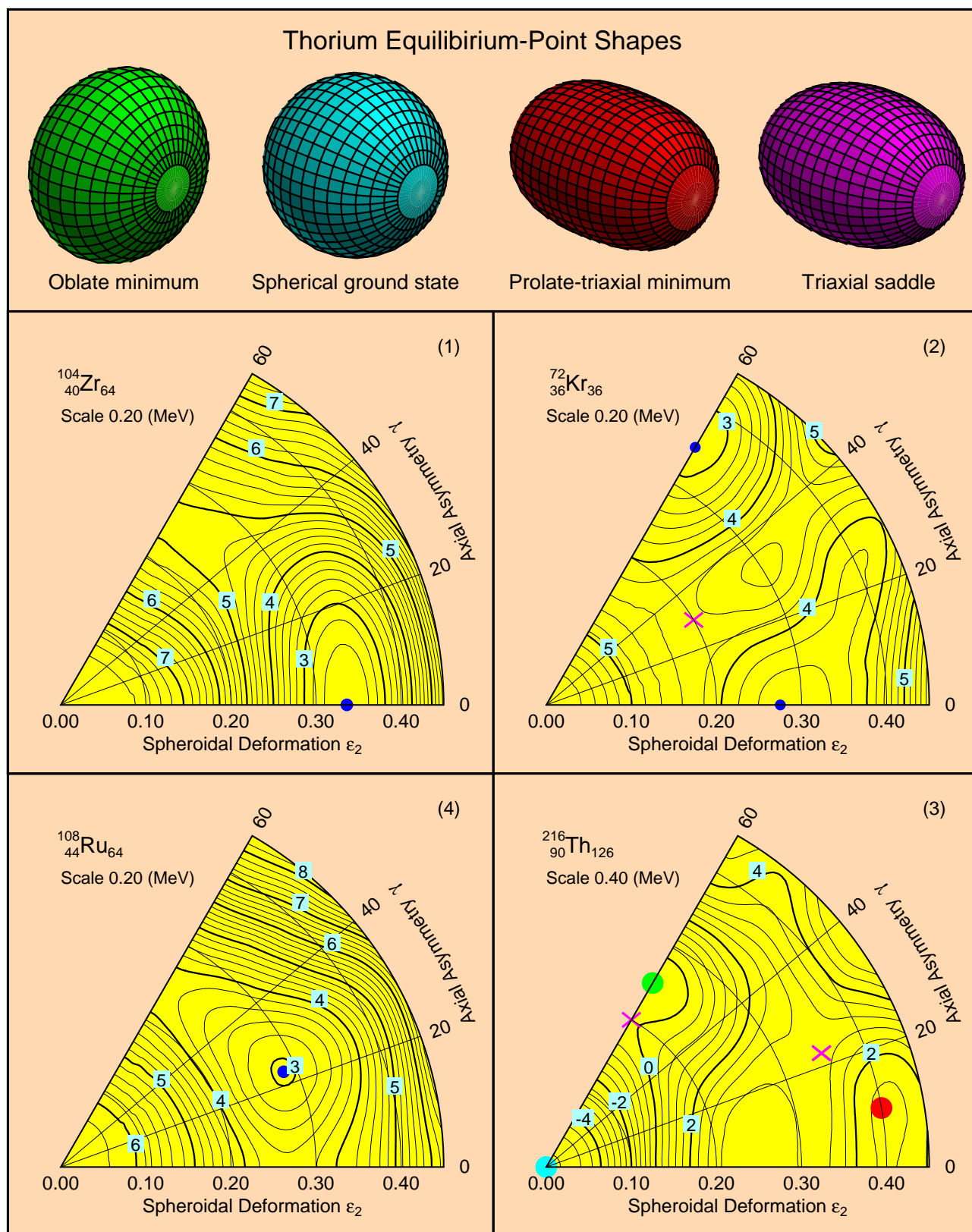
Although Table 1 extends over a larger region of the nuclear chart we limit the region displayed to regions where significant effects are found. Because we have recently increased the number of integration points in some calculations in our computer codes there are some (insignificant) differences between this Graph and the figure published in Ref. [10]. How our results relate to experimental data is discussed in Ref. [10].

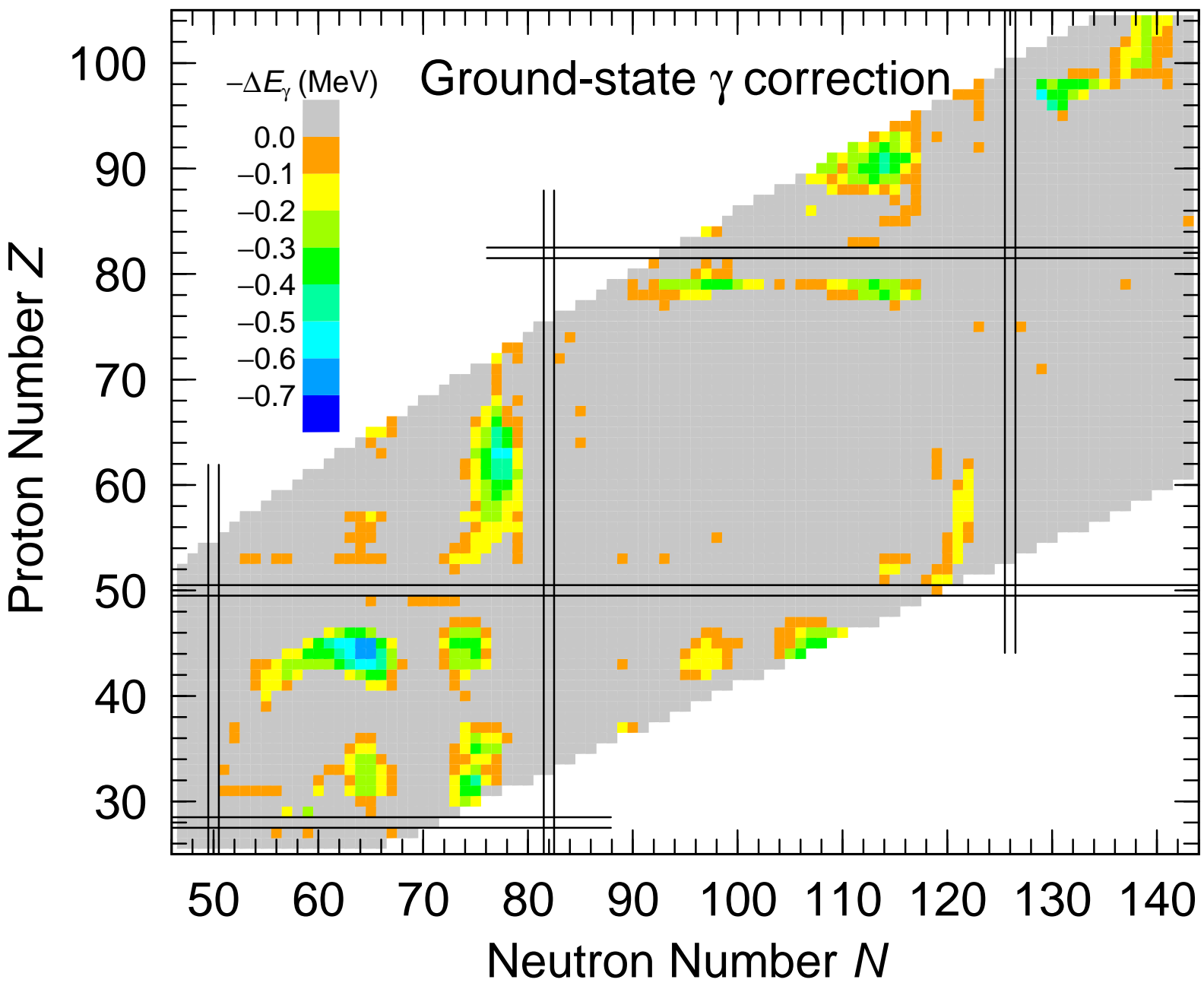
Graph 3 Calculated ground-state octupole instability for nuclei in the range  $47 < N < 143$ . Although

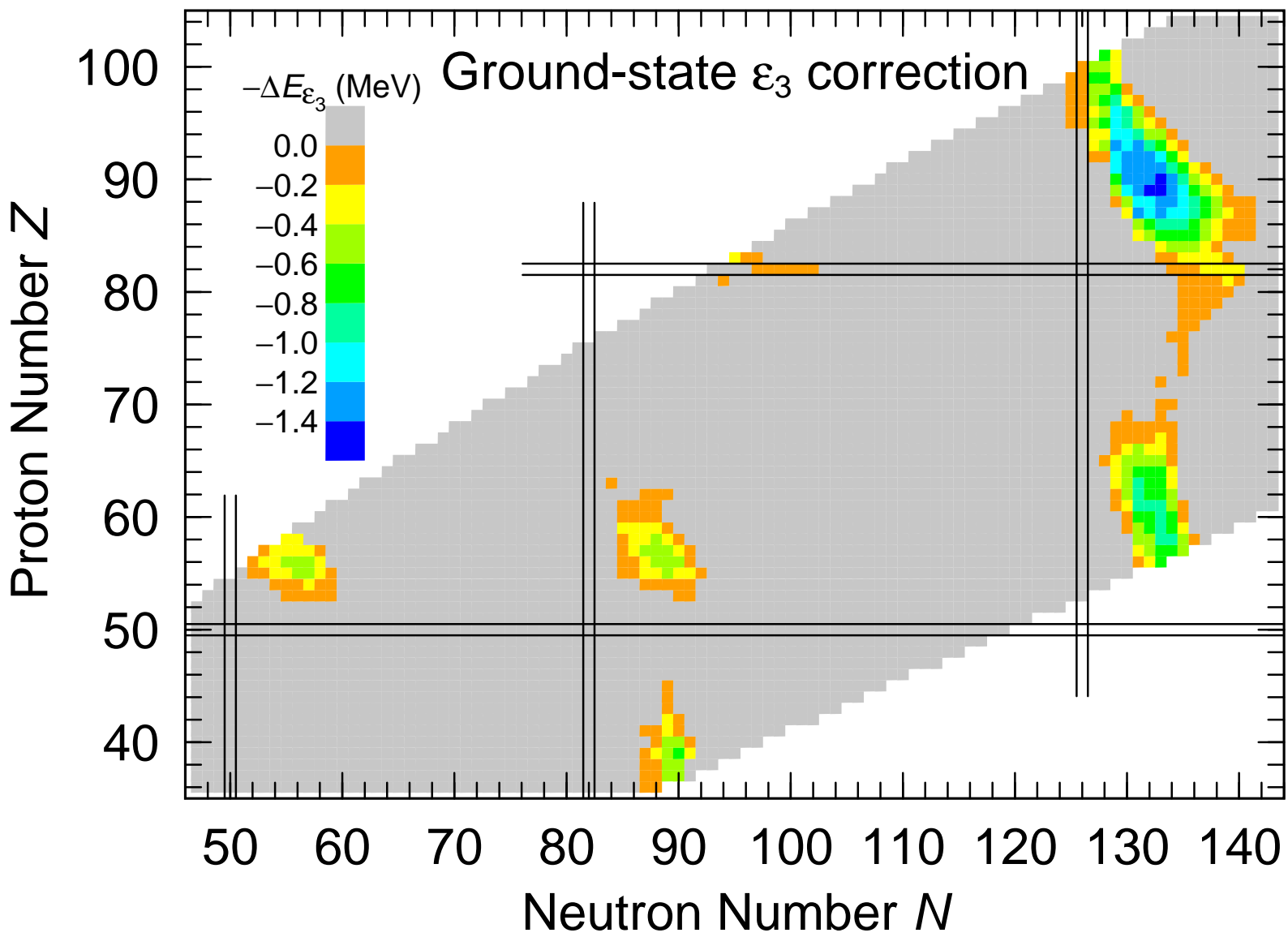
Table 2 extends over a larger region of the nuclear chart we limit the region displayed to regions where significant effects are found. Our calculations here are much more detailed than were possible in our mass paper published in 1995. Therefore there are some fairly significant differences between the calculated data in this Graph and figure 14 in Ref. [1]. The main difference is that for actinide nuclei the calculated region of octupole instability extends about three neutrons further away from  $N = 126$  than in [1].

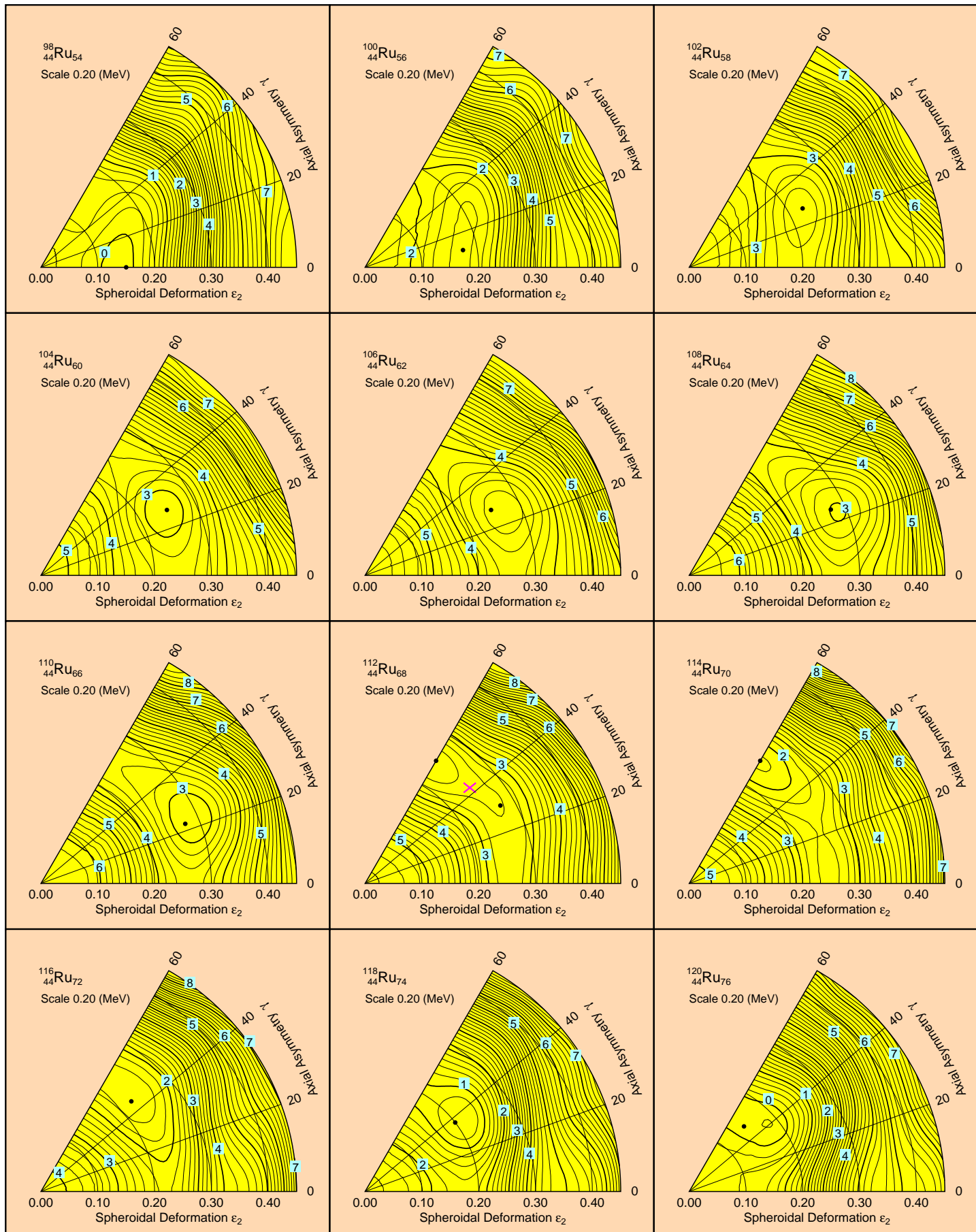
Graph 4 Twelve calculated potential-energy surfaces versus  $\varepsilon_2$  and  $\gamma$  (minimized with respect to  $\varepsilon_4$ )

for even Ru isotopes from  $^{98}\text{Ru}$  to  $^{120}\text{Ru}$ . The Ru isotopes from  $^{100}\text{Ru}$  to  $^{110}\text{Ru}$  are triaxial in shape. A less well established triaxiality reemerges at  $^{116}\text{Ru}$  but gradually fades away as  $N = 82$  is approached. For  $^{112}\text{Ru}$  and  $^{114}\text{Ru}$  the potential-energy surfaces are quite soft in the  $\gamma$  direction. If two minima are present the saddle between the minima is indicated by crossed lines, but only if the saddle is at least 0.05 MeV higher than the higher of the two minima, as is the case for  $^{112}\text{Ru}$ . For  $^{114}\text{Ru}$  the saddle at  $\varepsilon_2 = 0.25, \gamma = 20.0$  is less than 0.05 MeV above the prolate minimum at  $\varepsilon_2 = 0.25, \gamma = 0.0$ . Therefore the saddle and the prolate minimum are not marked.









Graph 4